HF CHAIN REACTION LASER

L. R. Boedeker, et al

United Technologies Research Center

Prepared for:

Office of Naval Research

May 1975

SECURITY CLASSIFICATION OF THIS PAGE (When Data Entered)

REPORT DOCUMENTATION PAGE

READ INSTRUCTIONS BEFORE COMPLETING FORM

1. REPORT NUMBER	2. GOVT ACCESSION NO.
3. RECIPIENT'S CATALOG NUMBER	AD A009 853
4. TITLE (and Subtitle)	HF Chain Reaction Laser
5. TYPE OF REPORT & PERIOD COVERED	Final Technical Report
6. PERFORMING ORG. REPORT NUMBER	R75-951883-4
7. AUTHOR(s)	L. R. Boedeker, J. F. Verdieck, R. J. Hall
8. CONTRACT OR GRANT NUMBER(s)	N00014-74-C-0379
9. PERFORMING ORGANIZATION NAME AND ADDRESS	United Technologies Corporation Research Center East Hartford, CT 06108
10. PROGRAM ELEMENT, PROJECT, TASK AREA & WORK UNIT NUMBERS	000173
11. CONTROLLING OFFICE NAME AND ADDRESS	Office of Naval Research Department of the Navy Arlington, VA 22217
12. REPORT DATE	May 1975
13. NUMBER OF PAGES	60
14. MONITORING AGENCY NAME & ADDRESS (if different from Controlling Office)	Naval Research Laboratory 4555 Overlook Avenue S.W. Washington, D.C. 20375
15. SECURITY CLASS. (of this report)	unclassified
15a. DECLASSIFICATION/DOWNGRADING SCHEDULE	

16. DISTRIBUTION STATEMENT (of this Report)

Distribution of this report is unlimited

17. DISTRIBUTION STATEMENT (of the abstract entered in Block 20, if different from Report)

18. SUPPLEMENTARY NOTES

19. KEY WORDS (Continue on reverse side if necessary and identify by block number)

kinetics of H_2/F_2 chain reaction

HF chain reaction laser

20. ABSTRACT (Continue on reverse side if necessary and identify by block number)

As a result of uncertainties in modeling reaction and molecular energy transfer processes in the cw H_2/F_2 chain reaction laser, UTRC has conducted a thermally initiated F_2/H_2 flow tube reactor experimental program to provide clearly defined experimental results via emission spectroscopy diagnostics on vibrational population levels attained in the cw H_2/F_2 chain reaction for comparison with theory. This experiment without the complexities of supersonic

(continued on back)

DD FORM 1 JAN 73 1473 E

SECURITY CLASSIFICATION OF THIS PAGE (When Data Entered)

flow, expansion through nozzles and power extraction provides information at this time on areas of major disagreement between theory and experiment and potentially will allow a more detailed comparison and adjustment of the pertinent rates. Highly dilute, subsonic, near room temperature reaction conditions in the 1-10 torr pressure region have been studied which result in development of the chain over flow tube distances of about 1 meter, much larger than mixing length. Fluorine is partially dissociated thermally and diluted with Ar and cold F_2. Subsequently H_2 with additional diluents is injected and mixed rapidly to start the chain reaction. Emission was observed through slotted windows along the reaction tube. Emphasis was placed on measuring the important high lying vibrational levels in HF, v = 3-6, via $\Delta v = 3$ overtone spectroscopy. An examination of the dominant kinetics operant in this region was conducted via the accumulation of spectral data over a range of key experimental parameters including distance from the H_2 injector, x; H_2 flow; F_2 flow; pressure; dissociator temperature, and O_2 additive flow. Reduction of $\Delta v = 3$ spectra shows consistent definition of a rotational temperature typically $T_R \sim 320^oK$, and at 5 torr a linear logarithmic-vibrational-level population variation with v indicating a vibrational temperature $T_v \sim 4300\text{-}6300^oK$. Increase in dissociator temperature was observed to cause an increase in vibrational populations as expected. A decrease in H_2 flow from $H_2/F_2 \sim 3$ to $H_2/F_2 \sim 1$ caused an increase in HF vibrational population which may arise from the effect of V-V relaxation of HF by H_2. At low pressure, $p \sim 1$ torr departures from a Boltzmann vibrational distribution were measured at x = 3 cm showing enhanced population of v = 5 and 6. Oxygen added with the cold F_2 that bypasses the dissociator had no noticeable effect, a result which suggests that once the chain reaction is started the oxygen either has little effect or O_2 contamination of F_2 is significant and little additional effect could be noted. At 5 torr and nominal flow conditions $F_2 \sim 1\%$, $H_2 \sim 3\%$, Ar ~ 96% populations on v = 3 and v = 6 were examined as a function of distance x from the H_2 injector. Results showed populations which decreased with x and level v. The available experimental results to data from the flow tube on high lying vibrational population distributions observed at 5 torr have been compared with predictions of the 1-D scheduled mixing analytical model in a manner which attempts to identify potential key areas of kinetic uncertainty with the chain. Results of this comparison suggest that (1) HF-HF VV and VT processes for high lying vibrational levels and (2) the overall rate of reaction and translational heating are two potential key areas of uncertainty. In particular, under (1) the observed distribution of vibrational level populations with level V could be explained to a large extent by a faster than linear HF VT scaling with V, perhaps as fast as V^3, whereas appropriate changes in back reaction or H_2 VV transfer mechanisms and/or rates in the model do not appear capable of explaining such level distribution data. Under (2) the observed spatial distributions of high lying HF vibrational populations and rotational temperatures suggest that propagation of the chain may be occurring somewhat slower than anticipated for present conditions.

UNITED TECHNOLOGIES CORPORATION
RESEARCH CENTER

Report R75-951883-4

May 1975

HF Chain Reaction Laser

Final Technical Report

by

I. R. Boedeker, J. F. Verdieck, R. J. Hall

Sponsored by

Department of the Navy
Office of Naval Research
Arlington Virginia 22217

CONTRACT NO. N00014-74-C-0379
NRL Req #00173-4-006331, 3-6-74

Monitored by

Naval Research Laboratory
Optical Sciences Division
Washington D.C. 20375

R75-951883-4

HF Chain Reaction Laser

Final Technical Report

Contract No. N00014-74-C-0379

TABLE OF CONTENTS

TABLE OF CONTENTS

LIST OF ILLUSTRATIONS

List of Illustrations (Cont'd)

LIST OF TABLES

HF Chain Reaction Laser

Final Technical Report

I. SUMMARY

The evaluation of the performance potential of the cw H_2/F_2 chain reaction laser is difficult due to the uncertainties in many of the chemical reactions, vibration-vibration transfer and vibration-translation relaxation rates. Considerable time and development of new techniques would be required to completely determine all these rates. As a result under the present contract UTRC has conducted a thermally initiated F_2/H_2 flow tube reactor experimental program to provide clearly defined experimental results via emission spectroscopy diagnostics on vibrational population levels attained in the cw H_2/F_2 chain reaction for comparison with theory. This experiment without the complexities of supersonic flow, expansion through nozzles and power extraction provides information at this time on areas of major disagreement between theory and experiment and potentially will allow a more detailed comparison and adjustment of the pertinent rates.

Highly dilute, subsonic, near room temperature reaction conditions in the 1-10 torr pressure region have been studied which result in development of the chain over flow tube distances of about 1 meter, much larger than mixing length. Fluorine is partially dissociated thermally in a nickel dissociator core heated inside a commercial tube furnace. The partially dissociated F_2 is then diluted with Ar and cold F_2. Subsequently H_2 with additional diluents is injected and mixed rapidly to start the chain reaction. Emission is observed through slotted windows along the reaction tube. Under the contract F_2 dissociator, F_2 dilution, H_2 injector and 5 cm dia. flow tube reactor apparatus components were designed, fabricated, assembled and tested. Overtone emission spectroscopy and F_2 uv absorption diagnostic equipment was assembled and measurements conducted. Emphasis was placed on measuring the important high lying vibrational levels in HF, v = 3-7, via $\Delta v = 3$ overtone spectroscopy. An examination of the dominant kinetics operant in this region was conducted via the accumulation of spectral and uv data over a range of key experimental parameters including distance from the H_2 injector, x; H_2 flow; F_2 flow; pressure; dissociator temperature, and O_2 additive flow.

The nickel dissociator has been heated up to an average measured temperature of $\bar{T} = 880^{\circ}K$ at a tube heater setting of $685^{\circ}C$; F_2 uv absorption data suggest an upper limit value for F_2 dissociation somewhat below the equilibrium value based on $\bar{T}$.

Stable repeatable overtone spectra were obtained at all viewing ports, located between x = 3 and 70 cm. Strong $\Delta v = 3$ bands have been observed corresponding to v = 3-0, 4-1, 5-2 and 6-3 P and R branch transitions. In addition $\Delta v = 4$ transitions

have been observed corresponding to v = 8-4. 7-3, 6-2, 5-1 and 4-0 transitions. Reduction of $\Delta v = 3$ spectra shows consistent definition of a rotational temperature, typically $T_R \sim 320^\circ K$, and at 5 torr a linear logarithmic-vibrational-level population variation with v was obtained indicating a vibrational temperature $T_v \sim 4300\text{-}6300^\circ K$. Orange/yellow/green visible emission has been observed at viewing ports in the present experiment, likely, at present temperature levels, due to emission from low J, $\Delta v = 5$ transitions; no visible emission has been observed from a viewing port upstream of the H_2 injector indicating little backstreaming.

Increase in dissociator temperature was observed to cause an increase in vibrational populations as expected. A decrease in H_2 flow from $H_2/F_2 \sim 3$ to $H_2/F_2 \sim 1$ caused an increase in HF vibrational population which may arise from the effect of VV relaxation of HF by H_2. At low pressure, $p \sim 1$ torr, departures from a Botlzmann vibrational distribution were measured at x = 3 cm showing enhanced population of V = 5 and 6. Oxygen added with the cold F_2 that bypasses the dissociator had no noticeable effect, a result which suggests that once the chain reaction is started the oxygen either has little effect or O_2 contamination of F_2 is significant and little additional effect could be noted.

At 5 torr and nominal flow conditions $F_2 \sim 1\%$, $H_2 \sim 3\%$, $Ar \sim 96\%$ populations on v = 3 through v = 6 were examined as a function of distance x from the H_2 injector. The effect of wall material was checked by installing a teflon liner inside the copper reaction tube. Results showed populations which decreased with x and level v. Results with teflon wall material showed a reduced drop off in populations with x compared to copper but essentially the same v distribution; while for temperature a slightly enhanced rate of growth of rotational temperature was indicated for teflon with less data scatter. These results suggest H atom interaction with the wall is a measureable effect here since at present the optical depth of field includes wall regions as well as the center part of the tube.

The available experimental results to date from the flow tube on high lying vibrational population distributions observed at 5 torr have been compared at this time with predictions of the 1-D scheduled mixing analytical model in a manner which attempts to identify potential key areas of kinetic uncertainty with the chain. Results of this comparison suggest that (1) HF-HF VV and VT processes for high lying vibrational levels and (2) the overall rate of reaction and translational heating are two potential key areas of uncertainty. In particular, under (1) the observed distribution of vibrational level populations with level V could be explained to a large extent by a faster than linear HF VT scaling with V, perhaps as fast as V^3, whereas appropriate changes in back reaction or H_2 VV transfer mechanisms and/or rates in the model do not appear capable of explaining such level distribution data. Under (2) the observed spatial distributions of high lying HF vibrational populations and rotational temperatures suggest that propagation of the chain may be occurring somewhat slower than anticipated for present conditions.

II. INTRODUCTION

The evaluation of the performance potential of the cw H_2/F_2 chain reaction laser is difficult due to the uncertainties in many of the chemical reaction, vibration-vibration transfer and vibration-translation relaxation rates. Considerable time and development of new techniques would be required to completely determine all these rates. In order to provide information in the near future, a flow tube experiment has been conducted under the reference Navy Contract to obtain information on the kinetics, and relaxation rates for comparison with the existing codes. This experiment, without the complexities of supersonic flow, expansion through nozzles and power extraction, potentially will allow a detailed comparison and adjustment of the pertinent rates and provides information at this time on areas of major disagreement between theory and experiment.

Flow tube experiments have provided a valuable approach for study of gas phase chemical reactions and molecular relaxation mechanisms. In the F_2-H_2 system a number of flow tube related experiments have been conducted to measure (1) reaction rates of F with H_2 and H with F_2 (Refs. 1 and 2); (2) distribution of vibrational-roational product states in these reactions (Refs. 3, 4, 5, 6); (3) HF-HF, VV, VT processes, HF-H_2, VV transfer and HF-H VT decay (Refs. 7, 8, 9). In these studies information on molecular energy transfer processes involving high lying vibrational levels V = 5, 6 is absent or appears uncertain. In addition in many of these studies, highly dilute discharge of H_2, F_2, or SF_6 in an inert gas are used for initiation, raising the possiblity that resultant energetic metastable atom populations are present (Ref. 10). These metastable atoms might conceivably interfere with the mechanism under investigation via metastable transfer collisions which here might result in F_2 dissociation or HF excitation. In studies involving discharged SF_6, S and SF_x species always are present adding additional uncertainty in evaluating basic chain reaction and relaxation phenomena. In the present flow tube chain reaction experiment spurious metastable and contaminant effects are avoided by dissociating the fluorine at low pressure in a thermal heater. The experiment is conducted at low pressure, low concentration of reagents, and low initial dissociation of F_2; under these conditions the chain reaction can develop uniformly in a subsonic flow with small temperature rise over a distance much longer than the time for mixing, thus tending to isolate the mixing process and control the heat release for study of basic processes, via accumulation of spectral data over a wide range of key experimental parameters, Table I.

With a thermal flow tube approach it was possible to devise a configuration which was compatible with state of the art F_2 uv absorption techniques (Refs. 11, 12), thus an attempt could be made to obtain F atom information by difference of F_2 absorption signals as dissociator temperature is increased. Alternative methods such as titration of resultant F/F_2 mixtures for F would be difficult because of possible confusion with F_2 reactions; direct ESR calibration of a flow tube would also be

TABLE 1

VERIFICATION OF MODEL

Select Run Conditions to Check the Various Kinetic Mechanisms

1. Back Reactions
    a. Stoichiometry, F_2
2. VV
    a. HF
    b. H_2
3. VT Rates
    a. Fctn. of V
    [b. T]
    [c. Atom Effects]
4. Chain Branching
    a. P
5. Chem. Kinetics
    a. He:Cd Laser Absorption for F_2

[6. Primitive Distribution]

Note: Items in Brackets Identified but Not Objective of Exploration in Present NRL Program

difficult because of geometry conflicts; hence these mthods were not considered in any detail here. Discharge dissociation of SF_6 to form S, SF_x and F species which could be titrated for F was not considered because of a desire as mentioned above to avoid S and SF_x contamination.

III. DESCRIPTION OF FLOW TUBE REACTOR EXPERIMENT

Approach

In order to obtain kinetic information for the cw H_2/F_2 chain reaction laser a thermally initiated flow reactor tube experiment has been conducted to study the population of vibrational levels in HF generated by the chain reaction of H_2 with F_2 employing spontaneous emission and F_2 uv absorption diagnostics (Fig. 1). Emphasis has been placed on measuring the high-lying vibrational levels in HF attained in the pressure region 1-10 torr via $\Delta v = 3$ overtone spectroscopy.

Apparatus

The experiments have been conducted in a 5 cm dia flow reaction tube with highly dilute mixtures of H_2 and F_2 in Argon, near room temperature and uniform subsonic flow conditions having a velocity $v \sim 10^4$ cm/sec. The chain is initiated in a controlled manner by thermal partial dissociation of F_2 at low pressure in a nickel core located inside a commercial tube furnace (Fig. 2). Changes in F_2 concentration in the dissociator are monitored via absorption of a uv probe laser to provide a check on the degree of dissociational equilibrium attained and the stability of F_2 flow conditions. Low overall F_2 concentration and near room temperature conditions are achieved by dilution with Argon diluent and additional cold F_2 injection. Angled injection of H_2 and additional Argon diluent through orifices in a row of small tubes acheives substantial mixing in about 5 cm (Fig. 3). Spontaneous emission from the reacting flow is monitored through slotted window ports at various stations along a 1 meter length of reaction tube. A viewing port just upstream of the H_2 mixer is provided to observe back streaming or back diffusion effects if any. F_2 dissociator, F_2 dilution, H_2 injector and flow tube reactor components were designed, fabricated and assembled under this contract study. A photograph of the assembled experiment is shown in Fig. 4.

Test Conditions

The flow tube reactor experiment is installed in one of the chemical laser labs at UTRC. This equipment has access to the 10 lb F_2 supply system in that lab via an inter-locked crossover control system. Metering of the F_2 flow is accomplished with pyrex tube rotometers and bellows sealed needle valve control. A sodium-bifluoride trap removes contaminant HF from the F_2 flow prior to the meters, cleaning the F_2 flow and preventing etching of the glass tubes. The experiment is connected to the mechanical vacuum pumping system for that lab, consisting of a 4000 CFM Leybold-Heraeus mechanical lobed impeller booster backed by a pair of 400 CFM Trochoidal

FIG. 1

$H_2 + F_2$ CHAIN REACTION LASER KINETICS EXPERIMENT

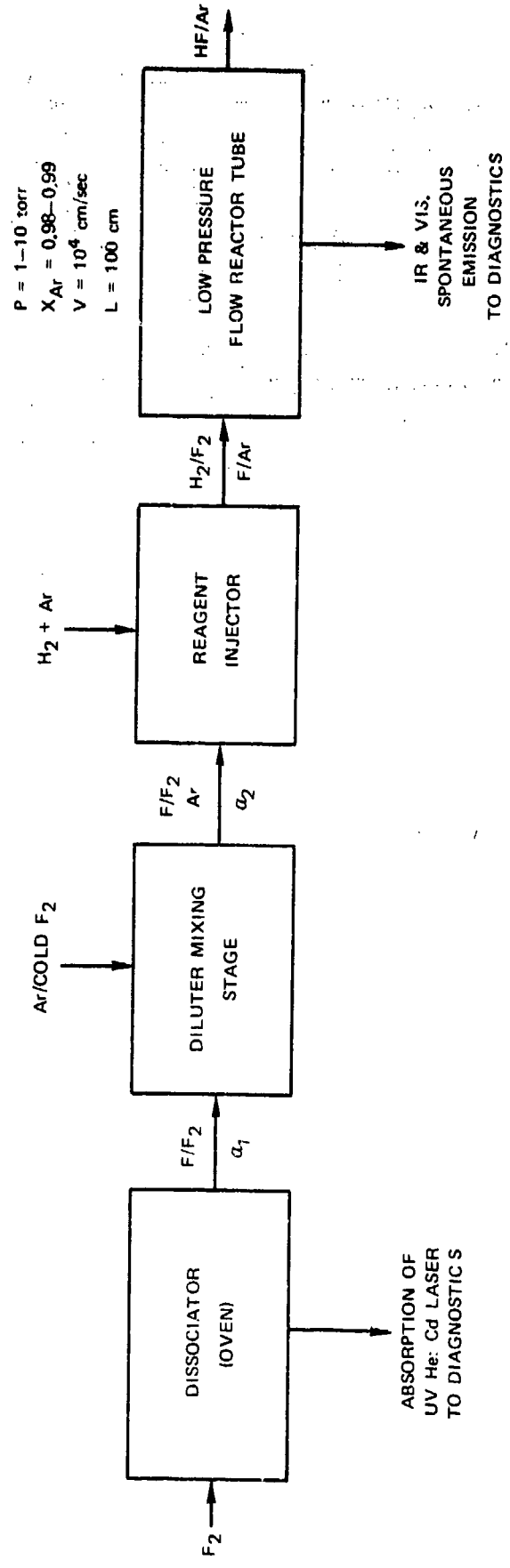

R04-2-1

FIG. 2

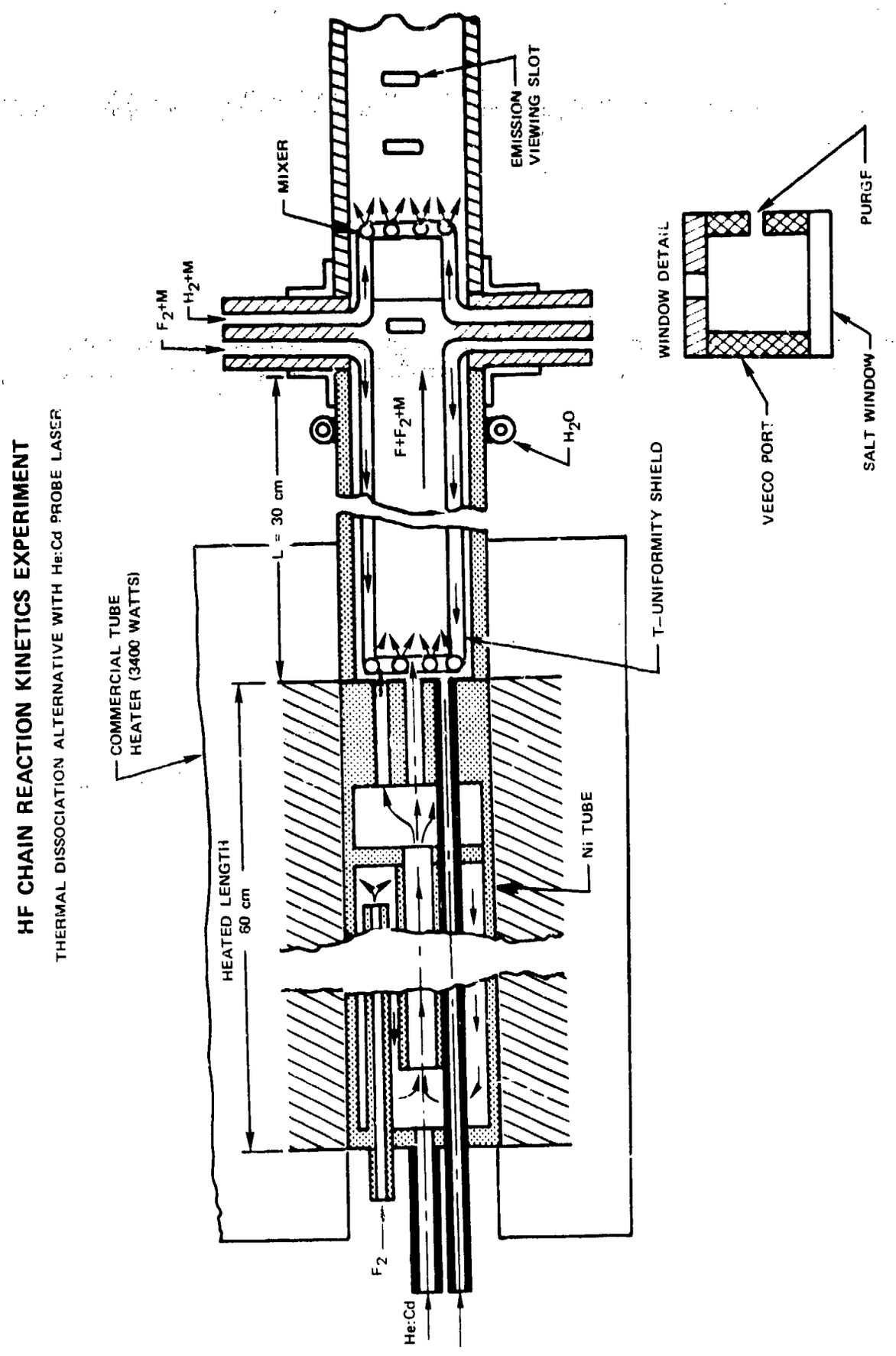
HF CHAIN REACTION KINETICS EXPERIMENT
THERMAL DISSOCIATION ALTERNATIVE WITH He:Cd PROBE LASER
EMISSION VIEWING SLOT
MIXER
F_2+M
H_2+M
H_2O
F+F_2+M
L = 30 cm
COMMERCIAL TUBE HEATER (3400 WATTS)
T-UNIFORMITY SHIELD
HEATED LENGTH 60 cm
Ni TUBE
F_2
He:Cd
WINDOW DETAIL
PURGE
VEECO PORT
SALT WINDOW

R04-2-9

FIG. 3

HF CHAIN KINETICS MIXER

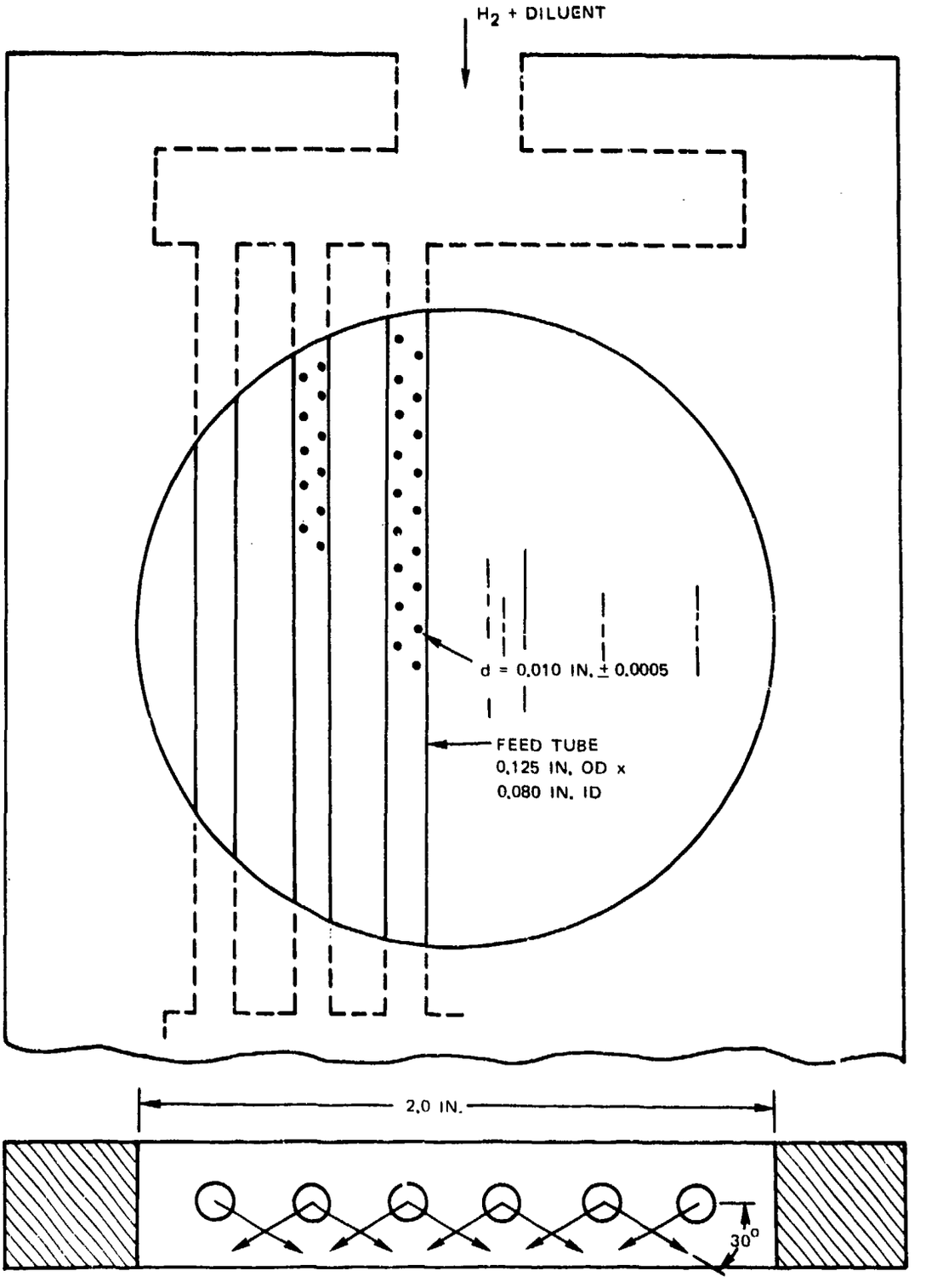

R04--2-8

FIG. 4

CW H_2/F_2 CHAIN REACTION FLOW TUBE EXPERIMENT

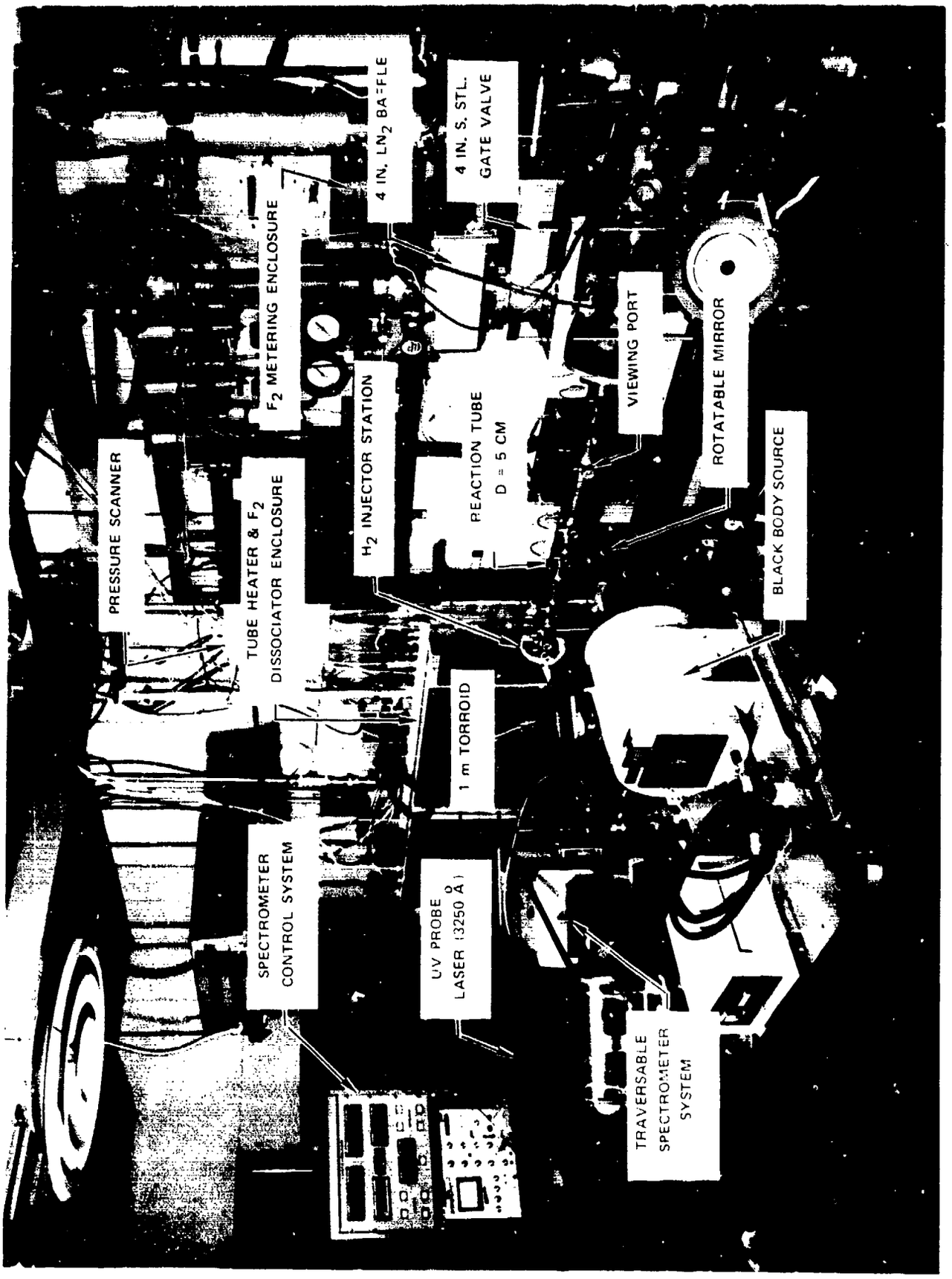

R04 2.5

pumps. The vacuum connection is made with a 4-in. line which provides about half of the system pumping capability at the experiment, adequate for pumping a 10 cm dia flow tube at a velocity of 10^4 cm/sec. Access to this vacuum line from the main vacuum line of the pumping system is via two 4-in. gate valves in series. A 4-in. chevron type LN_2 baffle between these valves provides cryogenically cooled isolation of the experiment from contaminants in the vacuum system. The large booster pump is used to outgas the experiment at dead ended booster pressures of about 10^{-4} torr; pumping of H_2O vapor and other condensables is then provided by the large in-line chevron baffle area. The F_2 supply and cw vacuum system are sufficient to provide long (several hours) test periods for gathering of spectral information.

Instrumentation and Equipment

Other components used in the experiment are a 4-ft x 12-ft optical table on which the experiment is assembled, a commercial 3.6 Kw regulated tube heater capable of temperatures up to 1200°C; a 12 port pressure scanning fluid switch for monitoring the pressure distribution in the experiment at several locations with a single transducer; and a Lyconix 3 mw uv probe laser (3250 Å) for F_2 absorption studies.

A spectral data acquisition system has been assembled for this experiment (Fig. 4). A 1/2 m Jarrell-Ash monochromator was used which has been provided at UTRC with a shaft encoder on the grating drive. A 6-in. dia 0.5 m focal length torroidal mirror is used for imaging. Spatial traversing capability of the spectral equipment on the 4-ft x 12-ft optical table is provided and access to a standard black body source is available at any spatial station via a rotatable mirror. A UTRC spectrometer control system (Fig. 4) was used for automatic acquisition of wavelength coded spectral intensity data in digital form using the above shaft encoder for a selected test condition; for most data it was sufficient to examine results in analog form on a strip chart.

IV. THERMAL DISSOCIATION OF F_2

Approach

It is desirable to operate the F_2 dissociator with high, near unity, F_2 mole fractions in order to minimize the heat transfer required to achieve a given gas temperature. Also this allows cooling of the gas by subsequent dilution for achieving the desired near room temperature fully diluted gas mixture at the H_2 injector. In addition, a low pressure level in the dissociator is desired to reduce the significance of volume recombination of F in the process of dilution of the hot dissociator F/F_2 effluent with cold inert gas and additional cold F_2. Then at 5-10 torr F_2 pressure, if the path length is a substantial fraction of a meter, it appears feasible based on prior studies, (Refs. 11, 12) to include a uv probe laser absorption diagnostic of F_2 in the dissociator to check on the disappearance of F_2 at high temperature levels due to dissociation.* The design of the dissociator (Fig. 2), was based on these criteria. The absorption of the uv by F_2 will occur primarily in the dissociator since the F_2 concentration in the rest of the beam path is very low, having been diluted rapidly at near constant pressure with inert gas. Any F atom information obtained from the uv absorption would be relevant to the F atom concentration at the H_2 injector since heavy species boundary layer growth in the F_2 dilution section will be small for planned flowrates at 5-10 torr and volume recombination of F should be slow.

F_2 Dissociation at Low Pressure

The equilibrium levels of F_2 dissociation in the 1-10 torr pressure region have been calculated using thermodynamic information available in the literature on F_2 (Ref. 13). Results (Fig. 5) show that substantial equilbrium dissociation levels can be achieved at low pressure below T = 1000°K. Such a temperature level is consistent with the strength and fluorine resistance properties of nickel, the material used to fabricate the dissociator.

At low pressure the time to reach dissociational equilibrium in F_2 can be long. Based on the known volumetric dissociation-recombination processes (Ref. 14) a linearized step by step solution for F-atom density $n_{F_{i+1}} = n_{F_i} + \delta n$ was devised.

---

*Such an absorption measurement here requires a resolution and stability of ± 0.25 - 0.5% in detecting probe laser intensity change which is difficult but based on the prior studies appeared to be a reasonable objective to accomplish.

FIG. 5

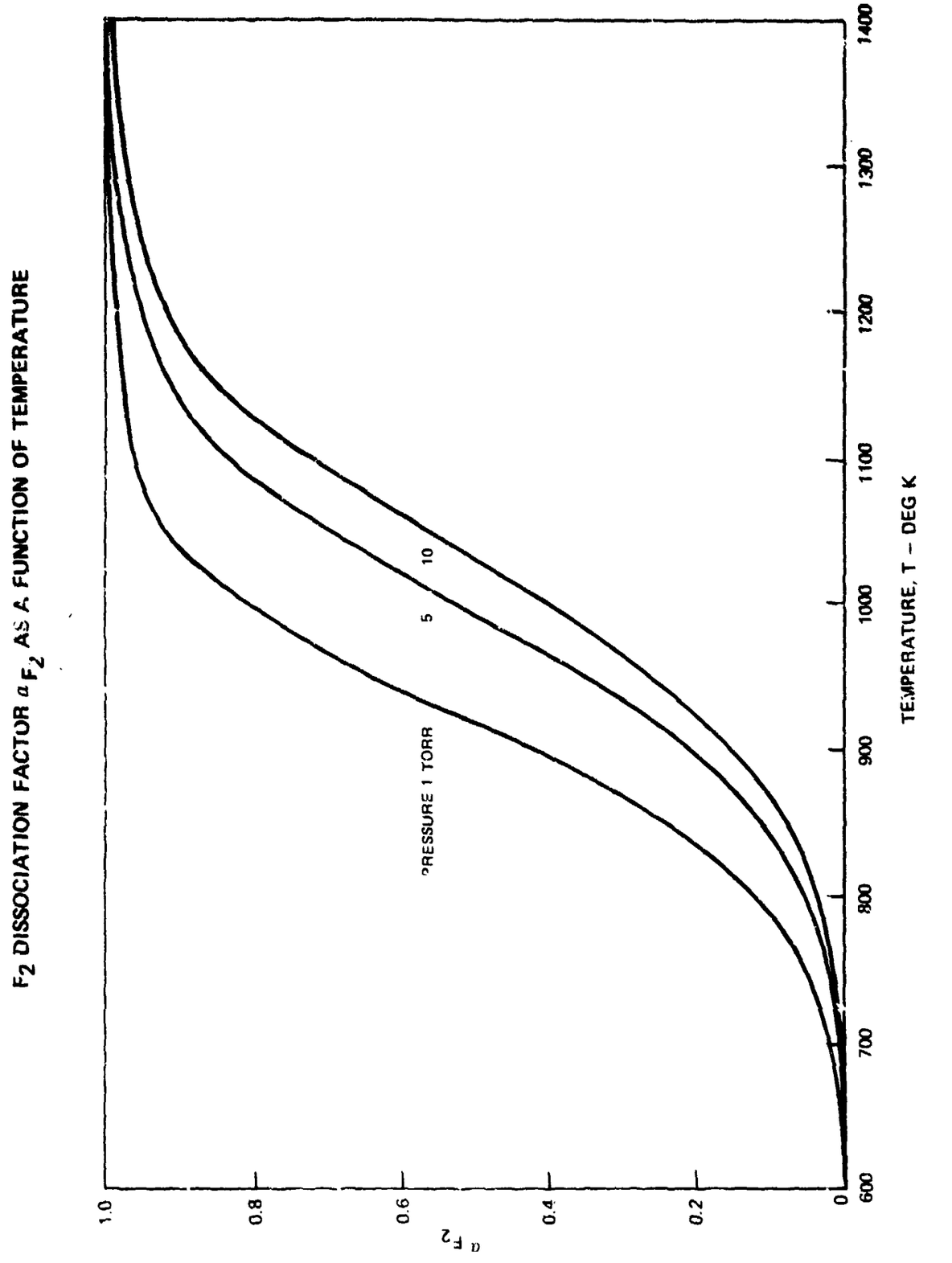
F_2 DISSOCIATION FACTOR α_{F_2} AS A FUNCTION OF TEMPERATURE
PRESSURE 1 TORR
5
10
α_{F_2}
0
0.2
0.4
0.6
0.8
1.0
600
700
800
900
1000
1100
1200
1300
1400
TEMPERATURE, T – DEG K

R05-84-2

A time to reach 90% of equilibrium F_2 dissociation at 5 torr for 1000°K, $\alpha_{eq} = 0.54$, of 10 seconds was calculated. At lower temperatures and/or pressures the time to reach equilibrium would increase further. The actual residence time in the dissociator at 5 torr for a 1% F_2 condition in the flow reaction tube will be less than 10 seconds; when all the F_2 flows through the dissociator the F_2 residence time in the dissociator is about 0.5 sec while if some F_2 is added after the dissociator with the dilution gas then the F_2 flowrate to the dissociator can be reduced and residence time increased to a limit here of about 5 sec.* Hence a true equilibrium condition would not be expected and surface effects likely will be significant. Experimental information on F/F_2 surface interaction is increasing, (Ref. 15), but at this time no attempt has been made to account for this. Rather it is expected that a stable repeatable value of F_2 dissociation will be achieved since temperature stability and repeatability can be obtained and long operating times are possible. Knowledge of the average absorptive properties of the F_2 in the final flow path through the dissociator via the uv absorption diagnostic then can provide valuable guidance, particularly in assigning at this time an upper limit to the level of dissociation actually achieved.

Temperature Levels and Distribution Measured in Dissociator

The actual temperature levels and distribution that have been achieved in the nickel dissociator with a 3 KW regulated commercial tube heater are shown in Fig. 6. It can be seen that good control of temperature level to the region of interest is possible, a maximum of 930°K having been achieved with about a 960°K(685°C) set temperature of the tube heater. Temperature gradients exist along the dissociator, however, about a 10% absolute difference in T between x = 0 and x = 12 as measured at r = 1" and 20% between x = 12 and x = 24 at r = 1; but only 10% between x = 12, r = 1 and x = 24, r = 0. Such gradients obviously would complicate the problem of predicting the dissociational performance still further here. It would be possible based on the above data to calculate the acial heat flux in the dissociator and to improve the temperature distribution by providing additional distributed heat addition. Heating tapes are already provided at the ends of the dissociator and it is likely that such additional heat addition would have to be more closely coupled thermally to the nickel. As long as sufficient F atoms are being produced it is not absolutely necessary to do this.

---

*A practical limit of about 5 sec to dissociator residence time will be set by a lower limit to F_2 flow rate through the dissociator below which uniform supply of hot F_2 to the dilution stage will not be maintained through the seven hole pattern, (Fig. 2); radial pressure gradients induced by the injected F_2 dilution gases can interfere with the distribution of subsonic flow through this pattern. For present operating points a special check was made on the radial pressure variation at the injector when no flow was present in the dissociator to insure that subsequent flow through the seven hole pattern would be relatively uniform.

FIG. 6

DISSOCIATOR WALL TEMPERATURE DISTRIBUTION

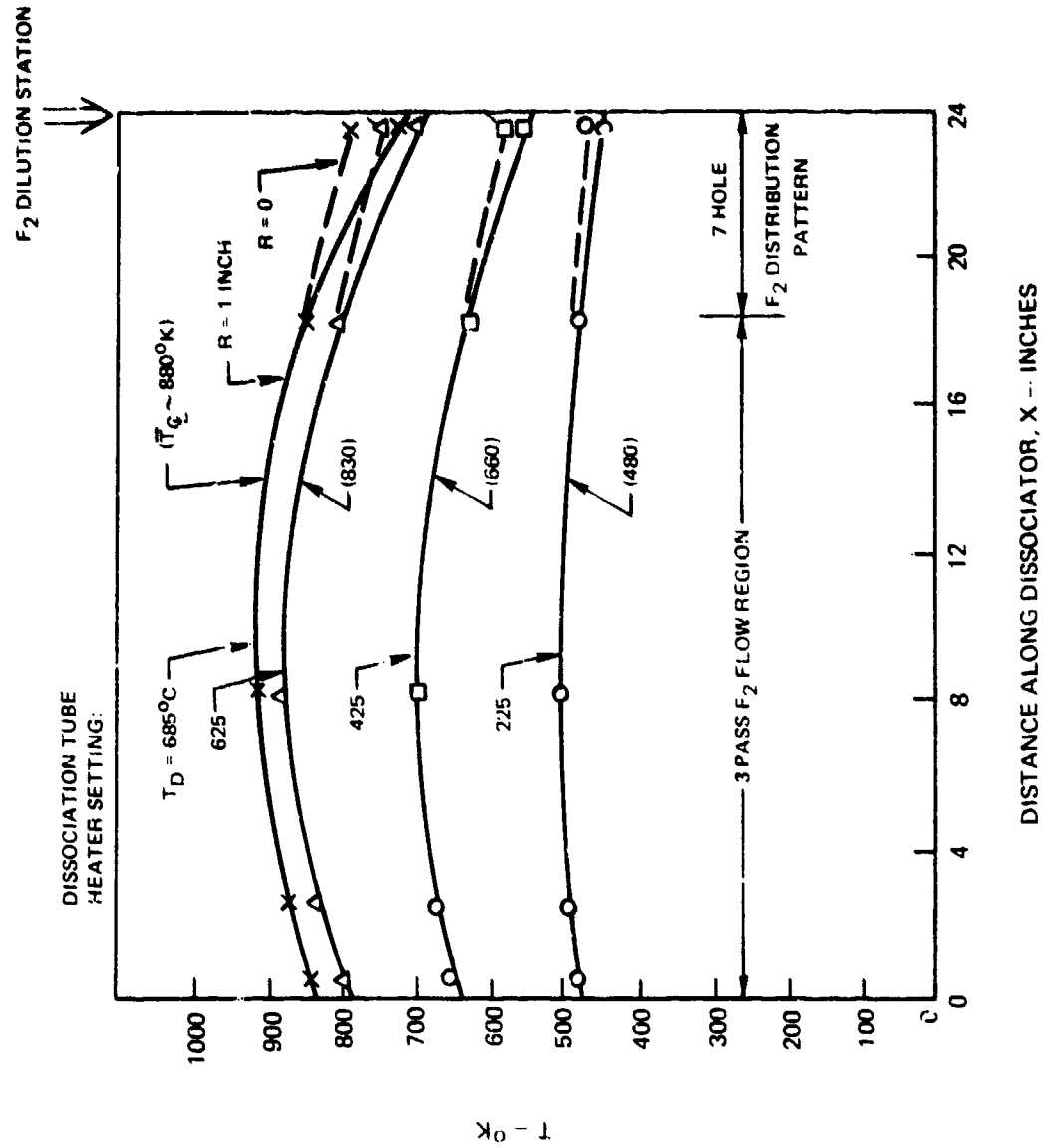

R05--57-1

V. MEASUREMENT OF F_2 UV ABSORPTION IN DISSOCIATOR WITH A 3250Å PROBE LASER

Approach

Two paths have been provided for uv laser probe beams through the dissociator (Figs. 2, 7). One path, for the primary probe beam, is along the center line of the dissociator, observing the F_2 flowing along a final pass through the dissociator in a 1/2" internal nickel tube. This beam passes through the center hole of the seven hole dissociator dilution feed section into the F_2 dilution region. Subsequently, the beam passes between the center two rows of tubing in the H_2 injector and is coupled out of the system through a quartz window after the reaction tube. A second probe laser beam path is through an internal bypass tube in the dissociator containing only purge gas; the probe laser beam along this path views only the diluted F_2 after the dissociator, i.e., the background signal level encountered also by the primary beam. Tests have shown that the absorption of this second background beam by diluted F_2 is indeed small as expected. Moreover, the primary beam absorption is not very sensitive to F_2 added after the dissociator in the dilution section confirming that the technique results primarily in observation of F_2 in the dissociator.

Temperature and Pressure Scaling of uv Data

Correlation of the F_2 dissociator uv absorption data to date has been attempted using the estimated average dissociator temperature values indicated for each tube heater temperature setting in Fig. 6. These values were obtained from a) the r = 1 data between x = 0 and x = 18 and b) the r = 0 data from x = 18 to x = 24. Here a) probably represents a good approximation to the actual temperature of the 1/2" internal nickel tube and F_2 gas between x = 0 and 18 and b) are actual wall and approximate gas temperature values. Viscous losses in pressure of the F_2 in the dissociator are generally small and at this time the pressure measured with a transducer at a wall tap located at x = 0, sensitive to the pressure of the F_2 entering the uv viewpath, has been used to correlate the data. Actually a small amount of measured Ar purge gas flow enters the dissociator at this point through a tube from the uv window region. This purge flow is generally less than 20% of the F_2 dissociator flow and is heated significantly in flowing along the hot window purge tube. The final data correlation has been made relative to the resultant partial pressure of F_2 in the viewpath.

F–ATOM DIFFERENTIAL ABSORPTION MEASUREMENT

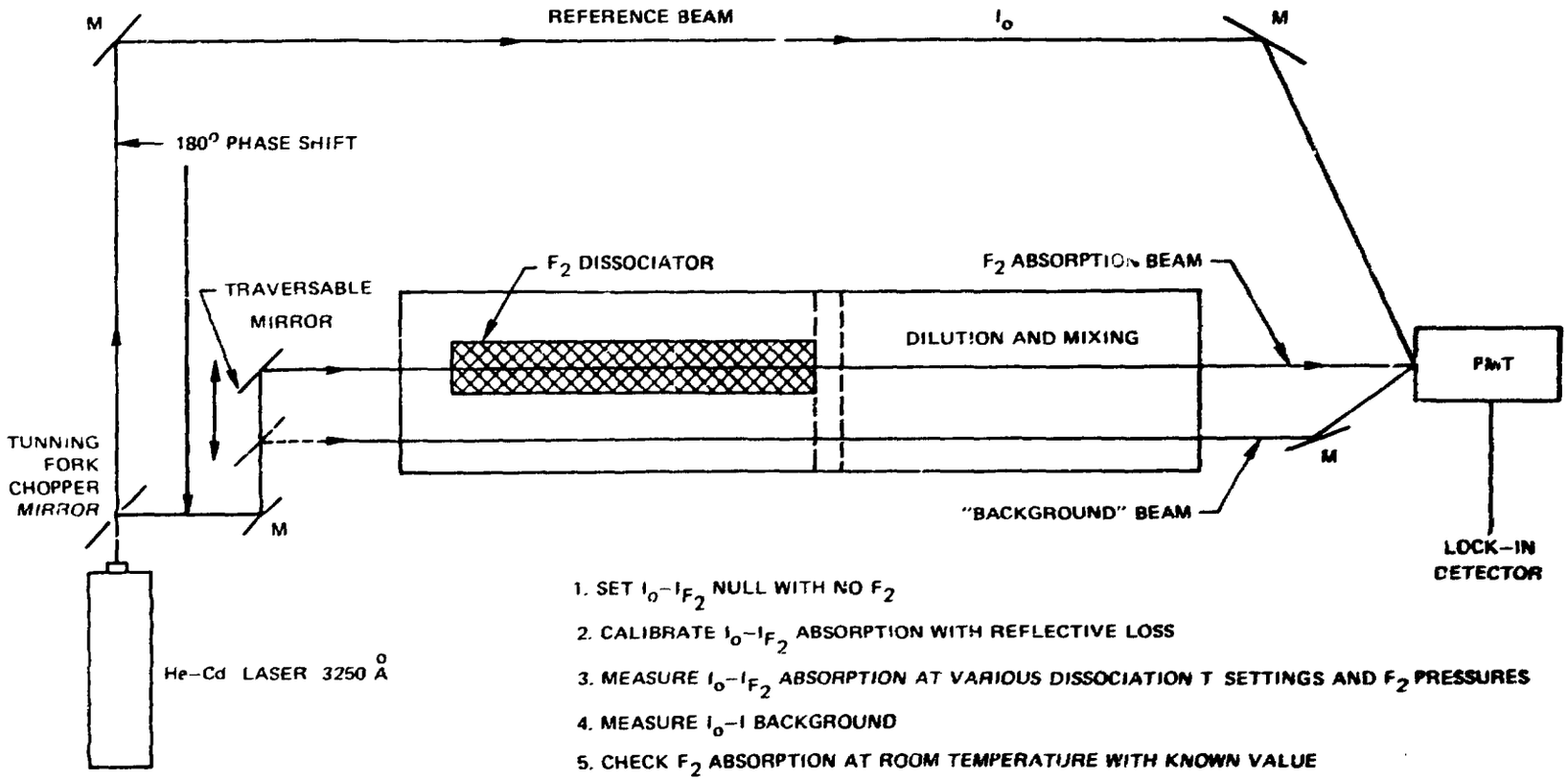

1. SET $I_o - I_{F_2}$ NULL WITH NO F_2
2. CALIBRATE $I_o - I_{F_2}$ ABSORPTION WITH REFLECTIVE LOSS
3. *MEASURE* $I_o - I_{F_2}$ *ABSORPTION AT VARIOUS DISSOCIATION T SETTINGS AND* F_2 PRESSURES
4. MEASURE $I_o - I$ BACKGROUND
5. CHECK F_2 ABSORPTION AT *ROOM TEMPERATURE WITH KNOWN VALUE*

Technique, Sensitivity, Stability

The differential absorption technique employed is shown in Fig. 7. A 400 Hz mirror chopper is used to provide 180° phase shifted probe and reference laser beams of almost equal intensity from the same source. The waveforms of probe and reference beams as viewed on an oscilloscope are quite similar but not square, a consequence of the mirror chopper oscillation amplitude being about equal to laser beam diameter. The beams are combined on an end-on photo tube (RCA 8575). Quartz lenses in each beam just before the photo tube (not shown in Fig. 7) are used to enlarge each beam spot size on the detector area to minimize nonlinear response. A check is made to ensure that the photo tube response is not sensitive to slight changes in beam position on the detector. A differential probe beam signal at 400 Hz is observed with a lock in amplifier and with no F_2 in the dissociator a null is achieved via slight adjustment of probe or reference beam intensities with adjustable irises (not shown in Fig. 7). Linearity was obtained by coupling the signals into the detector at reduced intensity off a quartz flat. With the laser (Lyconix model 303) adjusted for stable operation at about 2-3 mw output on a TM_{01} mode a system stability of $I/I_o \lesssim \pm 0.4\%$ over a time period of about 10-20 seconds was achieved sufficient to obtain some absorption information here by switching F_2 on and off. The stability determination was made by calibrating with a known reflective loss of about 8% (quartz flat) inserted in the probe beam near the detector. Linearity was demonstrated by inserting two quartz flats.

F_2 Absorption Results

Measurement of F_2 absorption at room temperatures in the dissociator indicated about a 12% absorption at 5 torr quite close to the level predicted for a path length of 60 cm based on existing extinction coefficient data* $\epsilon = 3.75$ ℓ/mole-cm at 25°C and 3250Å (Refs. 16, 17). The absorption data are obtained by switching the F_2 flow on and off. A long clearing time is required upon switching F_2 off and data points have been obtained only upon switching F_2 on after a stable initial signal was present. Absorption data α in % for various dissociator temperature and F_2 flow rate levels (dissociator pressure) are shown in Fig. 8. Values of α have been normalized with respect to measured F_2 partial pressure in the dissociator and the resultant data are correlated with the measured dissociator pressure for the various temperature levels set during the tests.

---

*Conversion of $\epsilon = 3.75$ to absorptivity yields a value $\alpha' = 4.6 \times 10^{-4}$ cm^{-1} $torr^{-1}$, differing by ℓn (10) with α' values used in Ref. 12.

FIG. 8

MEASURED F_2 ABSORPTION IN DISSOCIATOR AT 3250 Å

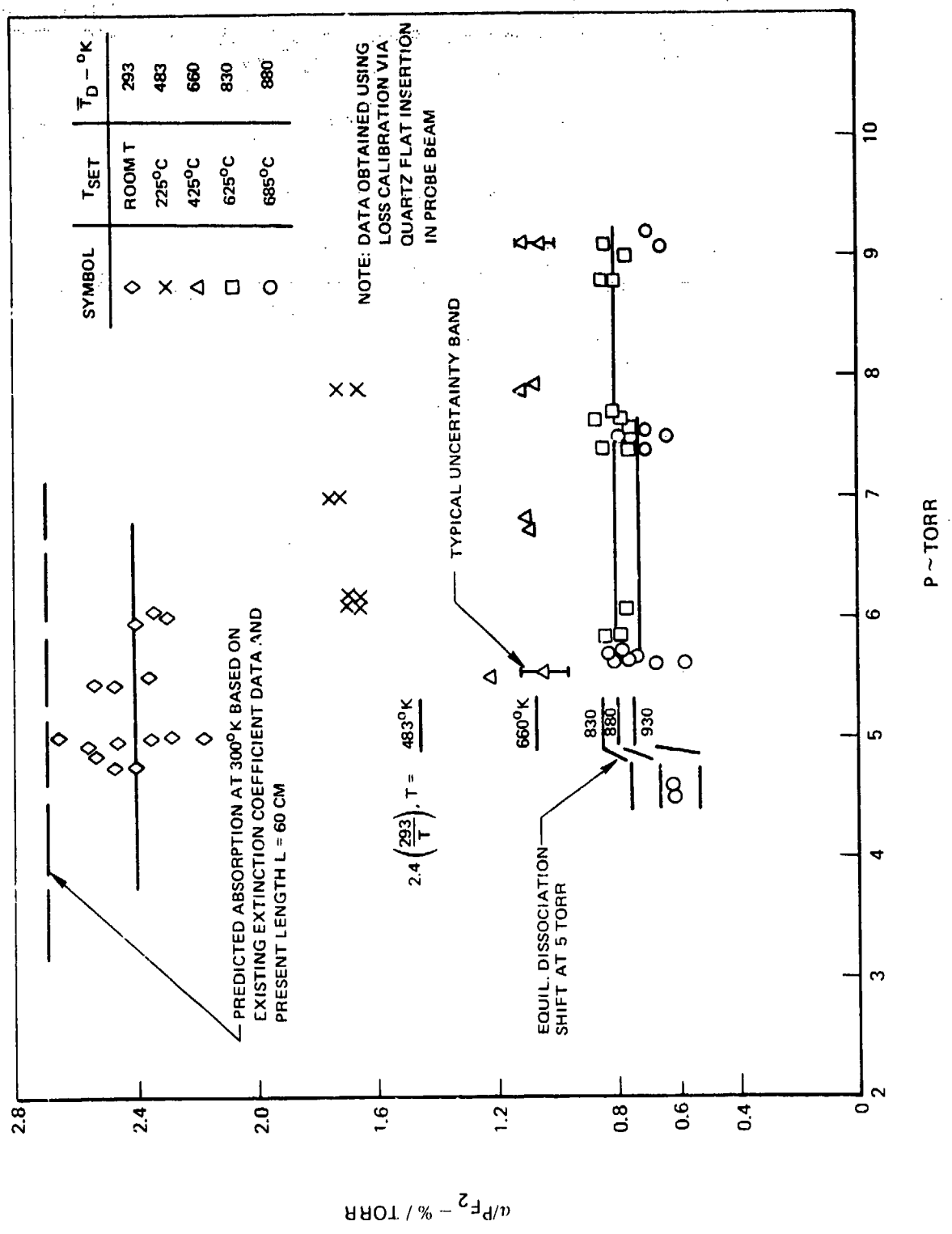

R05-57-2

There is more scatter evident in this data set than desired perhaps due to residual F_2 in the path prior to switching F_2 on. Results at lower temperatures for tube heater settings T_{set} = RmT, 225, 425°C, where little dissociation is expected indicate that the absorption is scaling correctly with pressure and indicate that the length of the absorbing column remains constant as F_2 flow rate is varied. In scaling with temperature the data for average dissociator temperature $\bar{T}_D$ = 660°K is quite close to a value scaled inversely with temperature (i.e., the change in density) from the room temperature data, while data at 483°K at this time appears high. Data for $\bar{T}_D$ = 830, 880°K fall below the inverse T scaling slightly. Data up to 100°C in Ref. 16 indicate little or no change in absorptivity with T for molecular F_2. The shift in absorption that would occur if equilibrium dissociation prevailed and F_2 absorption remains constant is shown in Fig. 8. An examination of the absorption expected for equilibrium dissociation at 930°K, the high temperature point achieved locally in the dissociator, suggests that the dissociation achieved is definitely below this level. The closeness of most of the $\bar{T}_D$ = 880°K data to the 830°K data suggests that less than equilibrium dissociation may prevail at $\bar{T}_D$. Further study is definitely needed but at this time an upper limit to F_2 dissociation somewhat below the equilibrium value at $\bar{T}_D$ is suggested. Because of the scatter of the present data the lower limit derived from the present results would be zero dissociation; hence suggesting that a separate calibration such as ESR to measure F directly and obtain a lower limit value would be useful for these conditions.

In much of the emission spectral data presented below, P was ~5 torr and the tube heater was set at T_{set} = 640°C. The ratio of F_2 bypassing the dissociator to dissociator F_2 flow was about 3. An upper limit of α_{F_2} = 2% is suggested by the uv data for these conditions.

VI. OVERTONE HF EMISSION SPECTROSCOPY RESULTS

Spectroscopic Measurements

Spectroscopic measurements were made of the $\Delta V = 3$ sequence of HF emission, extending from 8600 Å to 1.05 microns. The P and R branches of the $3 \rightarrow 0$, $4 \rightarrow 1$, $5 \rightarrow 2$, and $6 \rightarrow 3$ transitions were well resolved and the amplitude of individual rotational lines were measured. The system which measures this emission is described below, and the data reduction procedure is outlined immediately thereafter.

The chemiluminescent emission from excited vibrational states of HF in the reaction tube is collected through sapphire windows (which transmits visible to 6μ) by a six-inch gold toroidal mirror of one-half meter focal length. Two turning mirrors permit either this emission, or the emission from a Barnes Engineering black-body source, to be focused on the entrance slit of a 0.5 meter Jarrell Ash monochromator. The collected light is chopped by a PAR model 125 chopper at the entrance slit. The limiting aperture of the optical system is the monochromator aperture which is f:8.6. A 590 grooves/mm grating blazed at 6000 Å is used for this wavelength range. The detector employed is an EMI 9684B photomultiplier which has an S-1 photocathode spectral response. Although this type of tube is notorious for noise, it is the only type which covers the desired range. Noise is reduced by at least a factor of 100 by use of cooling to -60°C in a Products for Research cooled housing. The chopped signal is processed with a PAR HR-8 Phase Sensitive Detector and recorded on a 10-inch recorder. A typical spectrum of the $\Delta V = 3$ sequence is illustrated in Fig. 9. The $\Delta V = 4$ sequence has been recorded also, as shown in Fig. 10. Note that the $8 \rightarrow 4$ transitions can be observed, although not quantitatively measured.

The spectrometer system is calibrated with regard to sensitivity by recording the emission from the black-body source as a function of wavelength under carefully prescribed conditions and optimized optical alignment. This curve, when divided by the radiance, $N(\lambda)$, in watts/cm^2-Å-steradian, of the black-body source at the given temperature, defines the sensitivity of the spectrometer over the spectral slit width of the monochromator. Division by the spectral slit width (equal to the linear dispersion of the monochromator times the physical slit width) then yields the apparatus constant

$$C_{App} = \frac{\text{Black Body Response}}{N(\lambda) \cdot \text{Spectral Slit Width in Å}},$$

units of millivolts/watt/cm^2-steradian

C_{App} is plotted against wavelength at 100 Å intervals.

EMISSION SPECTRA FROM HF CHAIN REACTION

V = 3 SEQUENCE

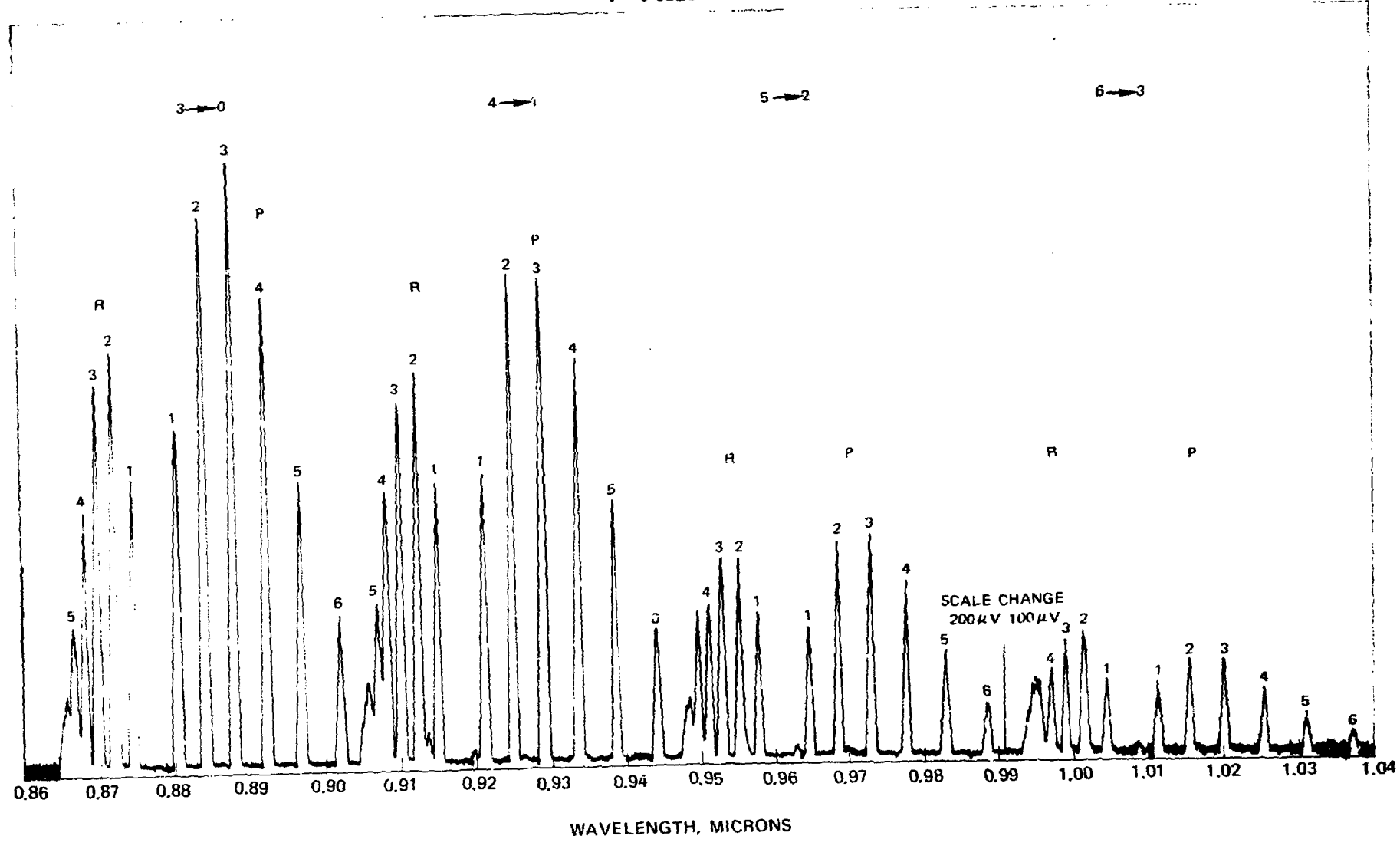

R03-207-6

FIG. 9

FIG. 10

EMISSION SPECTRA FROM HF CHAIN REACTION

$\Delta v = 4$ SEQUENCE

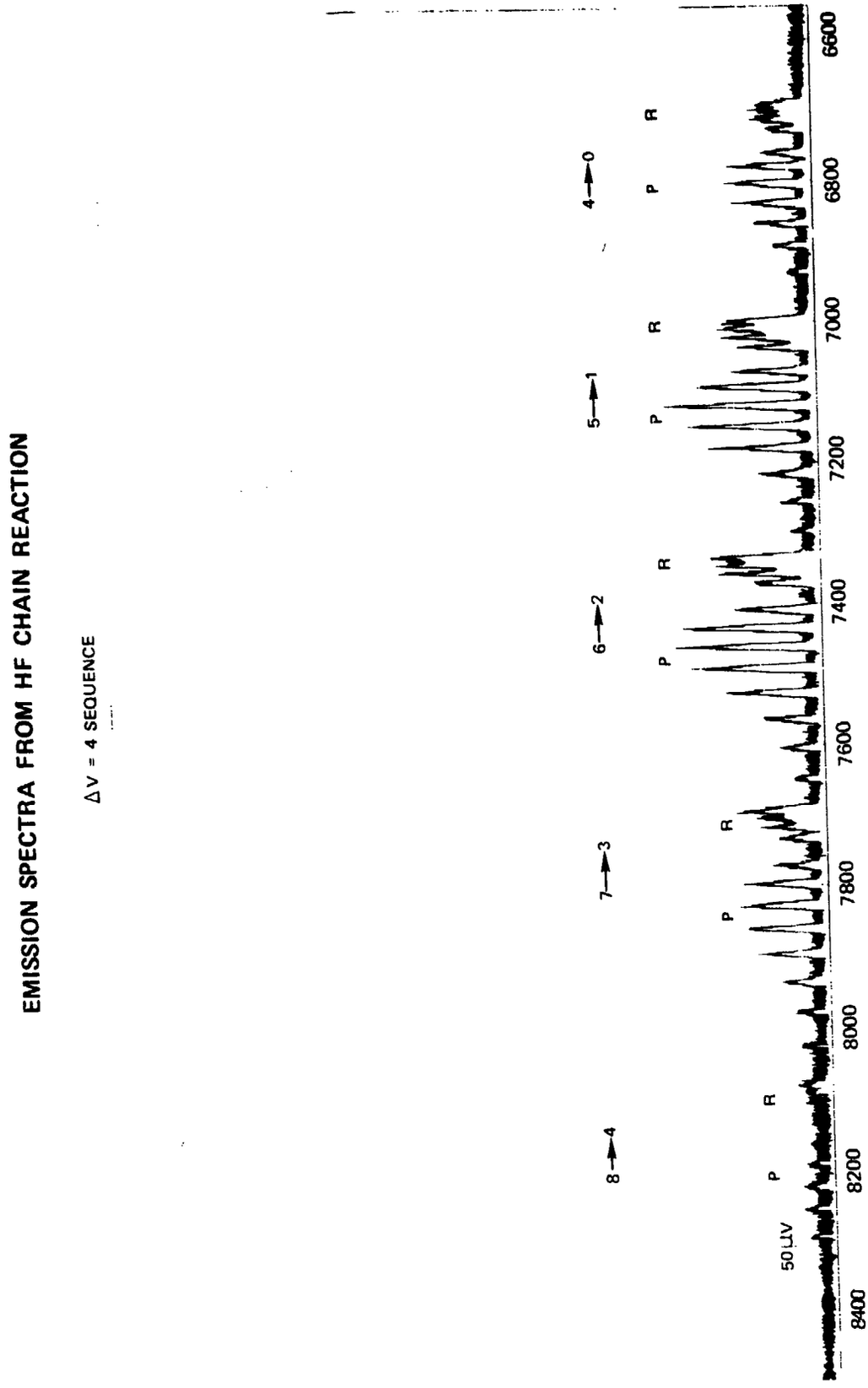

R03-207-4

The chemiluminescent emission from HF is recorded under conditions of slit width, detector sensitivity, optimum optical alignment, etc., so that the maximum signal is accepted from the reactor as was received from the black-body source. The recorded spectra are then identified by knowing approximate wavelength on the chart and by reading precise values from Meridith, Ref. 18, or from Proch and Wanner, Ref. 19. Identification is obvious for the $\Delta V = 3$ and $\Delta V = 4$ sequence transitions since these transitions are nonoverlapping and well-resolved as may be seen from Figs. 9 and 10. The P and R branch lines are identified and the peak heights are read and recorded in millivolts. For each line, the C_{App} value is taken from the C_{App} vs λ curve for the appropriate wavelength value and the peak height of the given line is divided by C_{App}. One now has the vibrational-rotational line absolute intensity in unit of watts/cm^2-steradian from which the vibrational population and the rotational temperature may be obtained.

The absolute intensities are given by the following formula

$$I = \frac{10^{-7}}{4\pi} h\nu c A_{VJ}^{V'J'} \frac{(2J'+1)}{Q_{ROT}^{V'}} \exp\left(\frac{-J'(J'+1)}{Q_{ROT}^{V'}}\right) N_{V'}[X]$$

the individual terms have the following meaning

10^{-7} converts watts to erg sec^{-1}

4π puts intensity on steradian^{-1} basis

h Planck's constant

$A_{V\ J}^{V'J'}$ Einstein coefficient for $V'J' \rightarrow VJ$ (taken from Gilleo, Ref. 20)

ν frequency in cm^{-1}

$Q_{ROT}^{V'}$ Rotational partition function for particular V' level of interest; here approximated by:

$$Q_{ROT}^{V'} = \frac{k\ T_{ROT}}{hc\ B_{ROT}^{V'}} = \frac{T_{ROT}}{1.43\ B_{ROT}^{V'}}$$

where the variation of $B_{ROT}^{V'}$ with V' must be duly accounted for.

If the equation is recast as

$$\frac{I}{\text{Denom}} = \frac{N_{V'}[X]}{Q_R^{V'}} \exp\left[-\frac{J'(J'+1)}{Q_R^{V'}}\right]$$

where Denom is $h\nu\, A_{V'J'}^{v'J'} \times \frac{10^{-7}}{4\pi}$

then the slope of I/Denom vs J'(J' + 1) yields $Q_{ROT}^{V'}$ (hence T_{ROT}), and $N_{V'}[X]$ may be found from the intercept. [X] is the depth of field of the light gathering system. For the 1M toroid, the depth of field is measured to be about 7.5 cm. Hence, the diameter of the reaction tube limits the path length over which emission is collected to 5 cm. In detail:

$$\ln I/\text{Denom} = \ln \frac{N_{V'}[X]}{Q_R} - J'(J'+1)/Q_R$$

$$\log I/D = \log \frac{N_{V'}[X]}{Q_R} - \frac{J'(J'+1)}{2.3Q_R}$$

$$\text{Slope} = -\frac{1}{2.3} Q_{ROT}^{V'} \qquad (\text{from } \text{Log}_{10} \text{ plot})$$

$$Q_{ROT} = -\frac{1}{2.3}\,\text{slope} \qquad T_{ROT} = Q_{ROT}^{V'} \times 1.43 \times B_{V'}$$

$$N_{V'} = \frac{\text{intercept} \times Q_{ROT}^{V'}}{[X]}$$

The $N_{V'}$ is determined, the vibrational temperature may be determined from a plot of I versus the vibrational quantum number V. A typical plot of the reduced intensity versus J(J+1) is shown in Fig. 11. A plot of vibrational populations against V is shown in Fig. 12. It is estimated that the derived quantities, T_R, $N_{V'}$ and T_V are accurate to about ±10%; however, a detailed error analysis has not been made yet. The major source of random error is from the reading of the peak heights of the vibrational-rotational lines. Systematic errors arise from nonoptimum alignment of the optical system and error in the temperature reading of the black-body source. A type of "theoretical" error arises from uncertainties inthe value of the Einstein coefficients.

Initial Experimental Results

Stable repeatable overtone spectra were obtained during initial tests at a viewing port 20 cm from the H_2 injector with 5 torr reaction tube pressure and dissociator temperature settings giving calculated (equilibrium) initial F_2 dissociation, α, in the range α = 1-5%. Strong $\Delta v = 3$ bands were observed corresponding to v = 3-0, 4-1, 5-2, and 6-3 P and R branch transitions. In addition $\Delta v = 4$ transitions were observed corresponding to v = 8-4, 7-3, 6-2, 5-1 and 4-0 transitions. Reduction of

FIG. 11

NORMALIZED INTENSITIES VERSUS ROTATIONAL ENERGY FOR PORT # 1

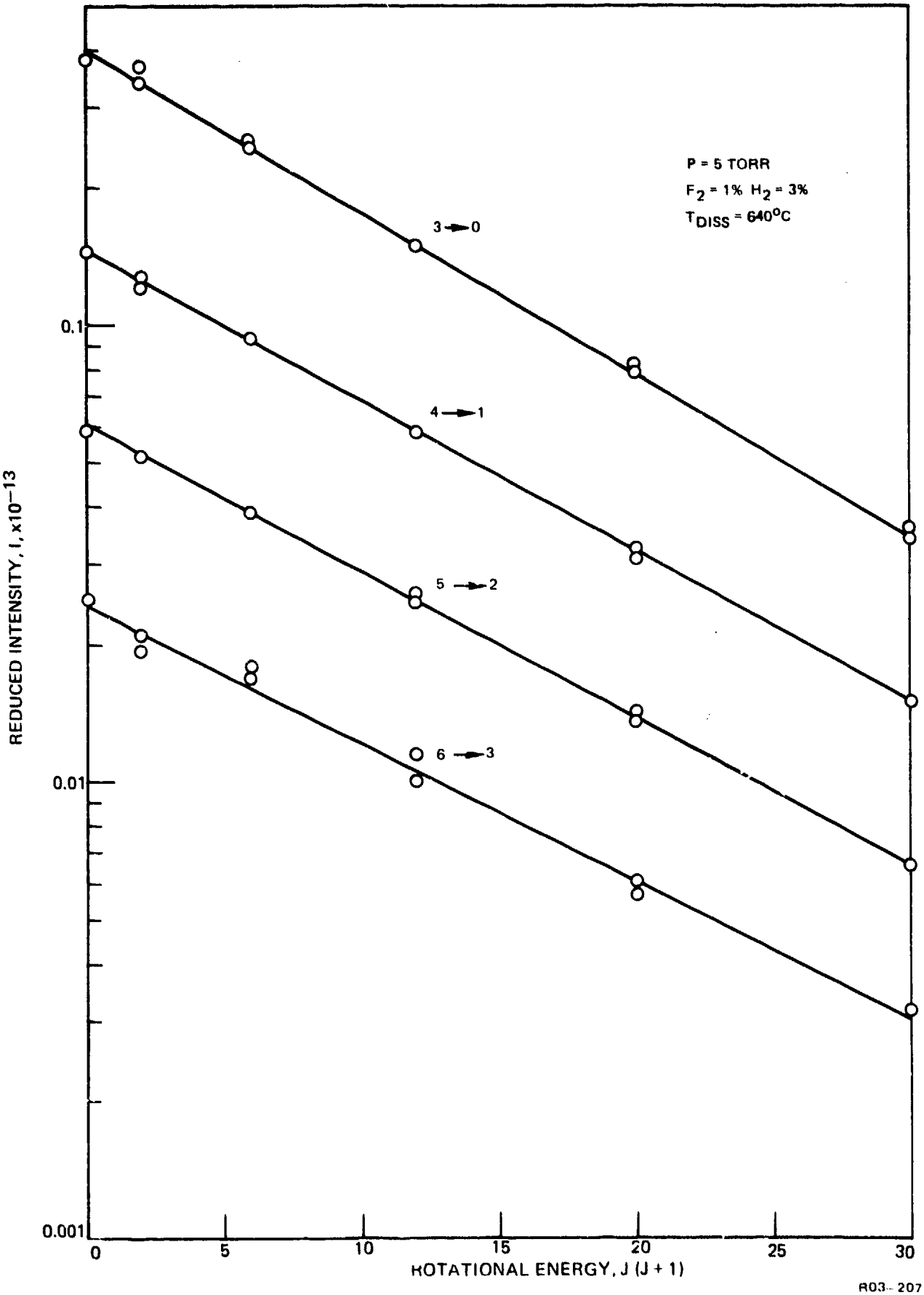

R03-207 2

$\Delta v = 3$ spectra showed consistent definition of a rotational temperature $T_R \sim 320°K$, and a linear logarithmic-vibrational-level population variation with v indicating a vibrational temperature $T_v \sim 4900°K$. These initial results suggested populations for $v = 3$ are of the same order as values predicted by the present UTRC 1-D scheduled mixing computer code and these measured populations fall off somewhat faster at higher V levels than predicted. These results at $x = 20$ cm corresponded to a flow time $\tau_f \sim 2$ ms, about a factor of 6 longer than reported in prior studies (Ref. 21). Orange/yellow/green visible emission was observed at other viewing ports in the experiment, likely due to emission from low J, $\Delta v = 5$ transitions. Yellow-green emission from the last port at $x = 90$ cm has been observed. With fixed F_2 flow through the dissociator the intensity of visible emission and overtone emission is observed to increase with increasing cold F_2 flow, a positive indication that the chain reaction is operative. No visible emission has been observed from a viewing port upstream of the H_2 injector indicating that backstreaming of H_2 does not occur significantly. Spectral data were obtained at $x = 20$ cm for two dissociator temperature settings, $T_D = 920, 980°K$; 2 values of H_2 flow, $H_2/F_2 \sim 3$ and $H_2/F_2 \sim 1$; and two Ar purity grades, 99.995 and 99.9999. Results appear particularly sensitive to H_2; are affected somewhat by dissociator temperature; while Ar purity has had no detectable effect on the observed spectra. F_2 uv absorption data at 3250 Å indicated the stable addition of F_2 to the dissociator at expected concentrations.

Distribution of Vibrational Level Populations with Distance

A baseline case of total pressure = 5 torr, $F_2 \sim 1\%$, $H_2 \sim 3\%$, Ar = 96% was used to examine the V = 3 through V = 6 populations as a function of distance from the mixer (hydrogen injector). These are nominal values of conditions; a calibration of all gauges has been made and exact values for tests are available. The thermal dissociation was set to 640°C. The linear flow velocity is nominally 10^4 cm/sec. The results--vibrational level populations, rotational temperature and vibrational temperatures--are tabulated as a function of distance in Table 2. Good reproducibility is indicated by the two entries for 40 cm, obtained on different days. The experimentally observed vibrational level populations are presented in Fig. 13. The rotational temperature estimated from this data are reasonable, considering the high dilution of room temperature argon. Typical plots for determining N_V and T_R were given in Fig. 11. For all distances along the flow tube for this baseline case, a Boltzmann distribution of vibrational levels was observed; an example was shown in Fig. 12. The slow cooling of the vibrational temperature, see Table 2, is indicative of some slow relaxational process; radiation losses, and VT collisional losses occurring at these low partial pressures of the H_2, F_2 and HF.

These experimental results are not in agreement with predictions of the existing model in that the model tends to predict more nearly constant values of level population along the tube and a nonBoltzmannian vibration level population distribution at higher v levels. Some basic features of the analytical results are discussed in a subsequent section of this report.

TABLE 2

VIBRATIONAL LEVEL POPULATION AS A FUNCTION OF DISTANCE FROM MIXER

ΔV=3 Sequence

Nominal Conditions: P_{tot} = 5 torr, H_2 = 3%, F_2 = 1%, T_{Dissoc} = 640°, v = 10^4 cm/sec

Nominal Distance cm	3	7	11	20.5	40	40[d]	70[d]
vibrational level	[a]						
3	1.01	1.02	.73	.53	.35	.36	.185
4	.38	.38	.28	.17	.090	.10	.048
5	.165	.16	.11	.061	.035	.034	.017
6	.069	.074	.05	.026	.016	.014	.007
$(T_R)_{ave}$ [b] (°K)	325	327	330	337	331	338	340
T_v [c] (°K)	6330	6020	6080	6120	4310	4720	2900

a. Units are 10^{13} molecules/cc
b. Average of 3 → 0, 4 → 1 values, probable error is less than 10%
c. from N_v vs V, probable accuracy ± 10%
d. data collected on a different day

FIG. 12

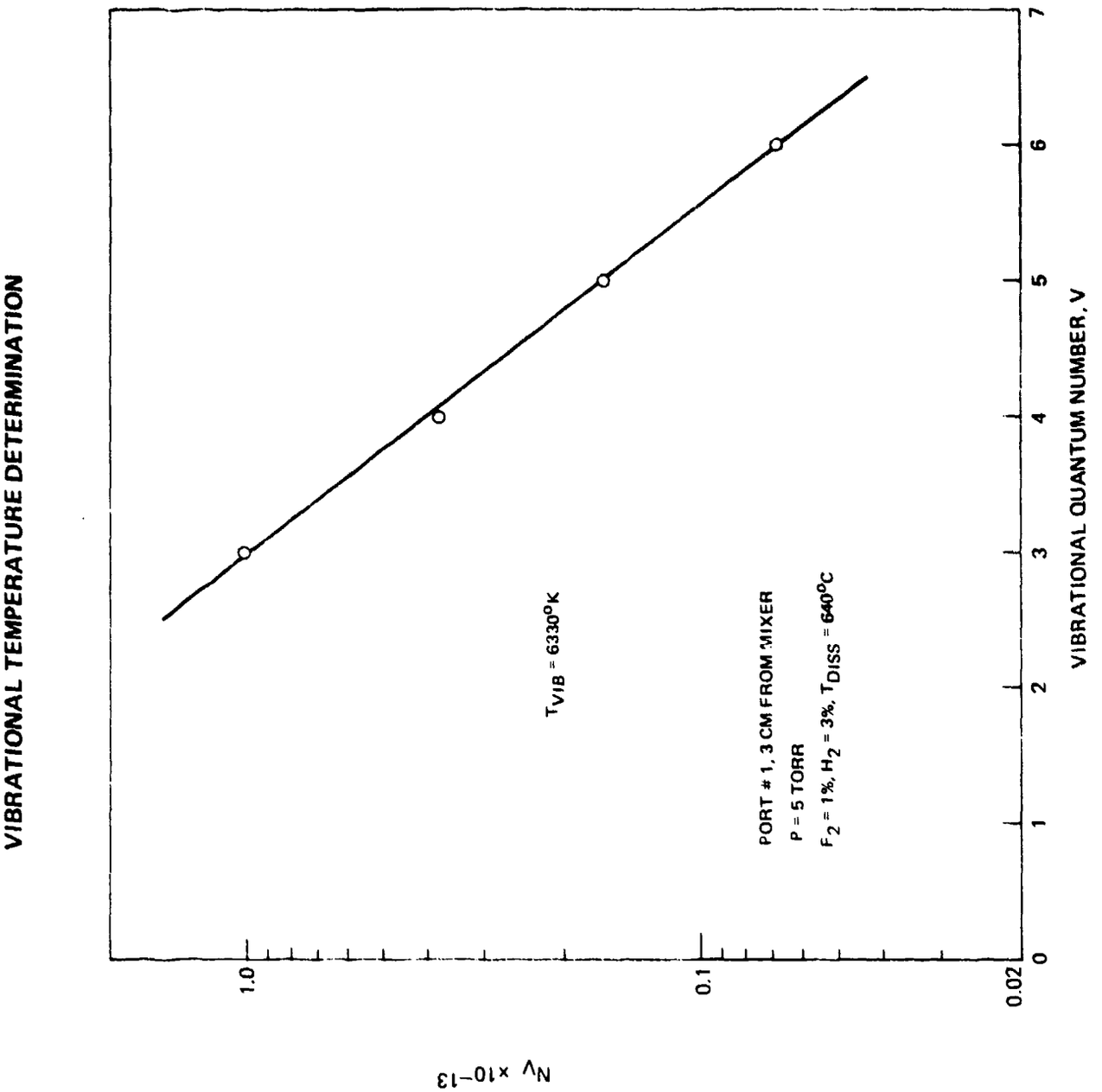

R03-207-6

FIG. 13

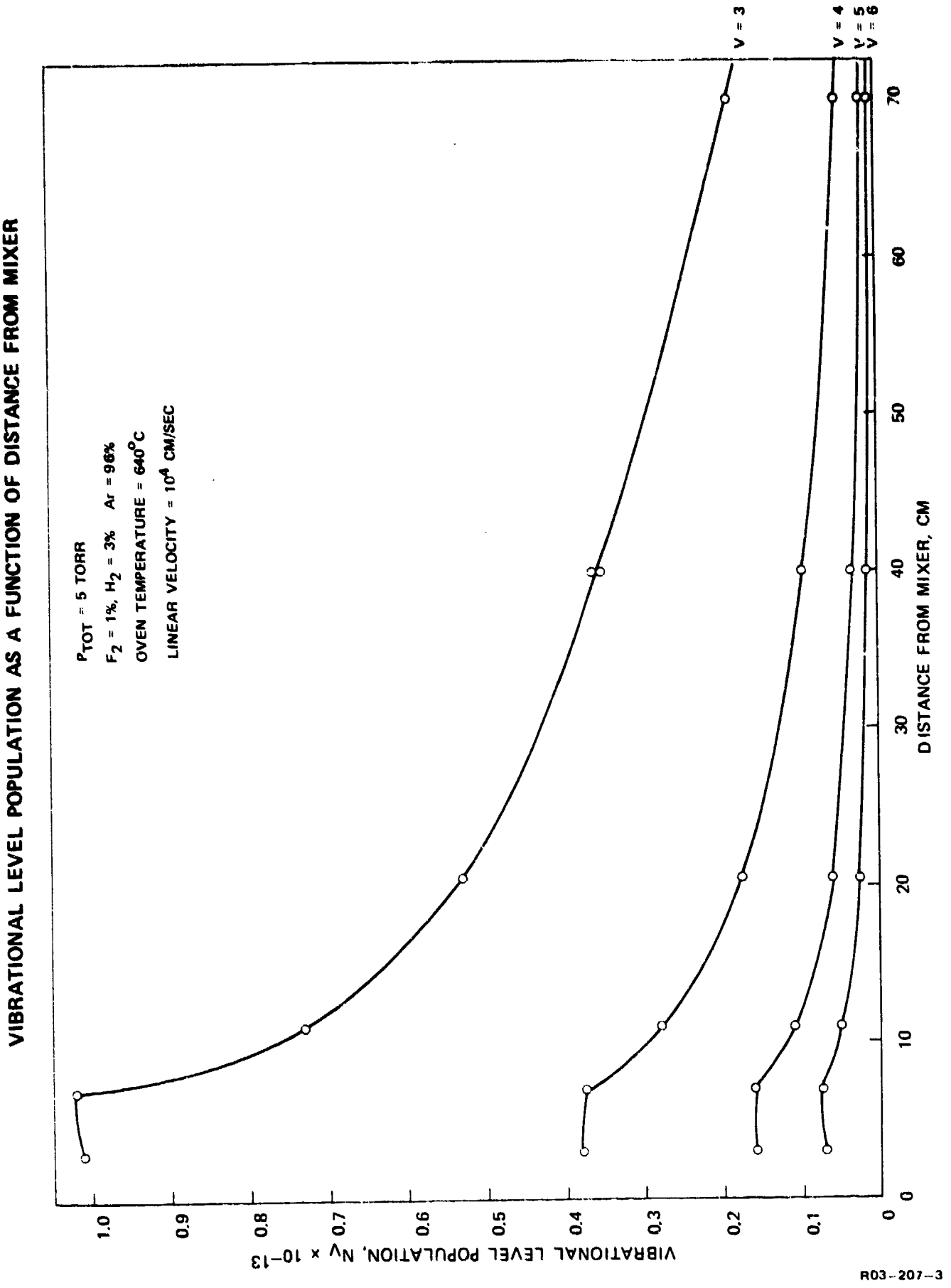

R03-207-3

Effect of Dissociator Temperature and H_2 Flowrate

Table 3 shown below, presents the effect of increased dissociator temperature and also the effect of decreased H_2 flow (providing stoichiometric H_2/F_2). These data were taken by viewing emission from one port only. The increase in vibrational populations is due to the increased degree of dissociation of F_2 exiting the dissociator. The increase in vibrational population from the decrease in H_2 flow may arise from the effect of reduced VV relaxation by collisions with H_2 molecules. However, this is not a conclusive result and further study is definitely called for.

Table 3

Vibrational Level Populations as a Function of Temperature and H_2/F_2 Stoichiometry

T, °C	625	685	685 (reduced H_2 flow)
V=3	.86	1.07	1.5
4	.26	.30	.39
5	.090	.10	.12
6	.040	.041	.052

units: 10^{+13} molecules/cc

Oxygen Effect

The addition of oxygen with the cold F_2 that bypasses the dissociator had no noticeable effect. Oxygen up to 50% of the F_2 flow was investigated, and there was no obvious change in the amplitude or distribution of the spectral lines. This preliminary result indicates that once the chain reaction is started, the oxygen inhibition has little effect. However, if O_2 contamination of F_2 is significant to begin with, then a saturation effect of O_2 on inhibition may occur (Refs. 22, 23) and the conclusion stated here is tentative.

Low Pressure Results

Some interesting results were obtained at low pressure, P ~ 1 torr. The vibrational distrubutions for 3 different cases are shown in Fig. 14. These cases are as labeled with nominal conditions. A. P_{tot} = 1 torr, ~ 1% F_2, ~ 3% H_2, T_{DISS} = 590°C: B. Conditions held constant, but cold F_2 diluent increased by a factor of 2; C. Conditions held constant, F_2 flow through dissociator decreased by a factor

VIBRATIONAL POPULATION DISTRIBUTION AT LOW PRESSURES

F_2 = 1%

H_2/F_2 = 3%

Ar = 96%

EXPERIMENTAL

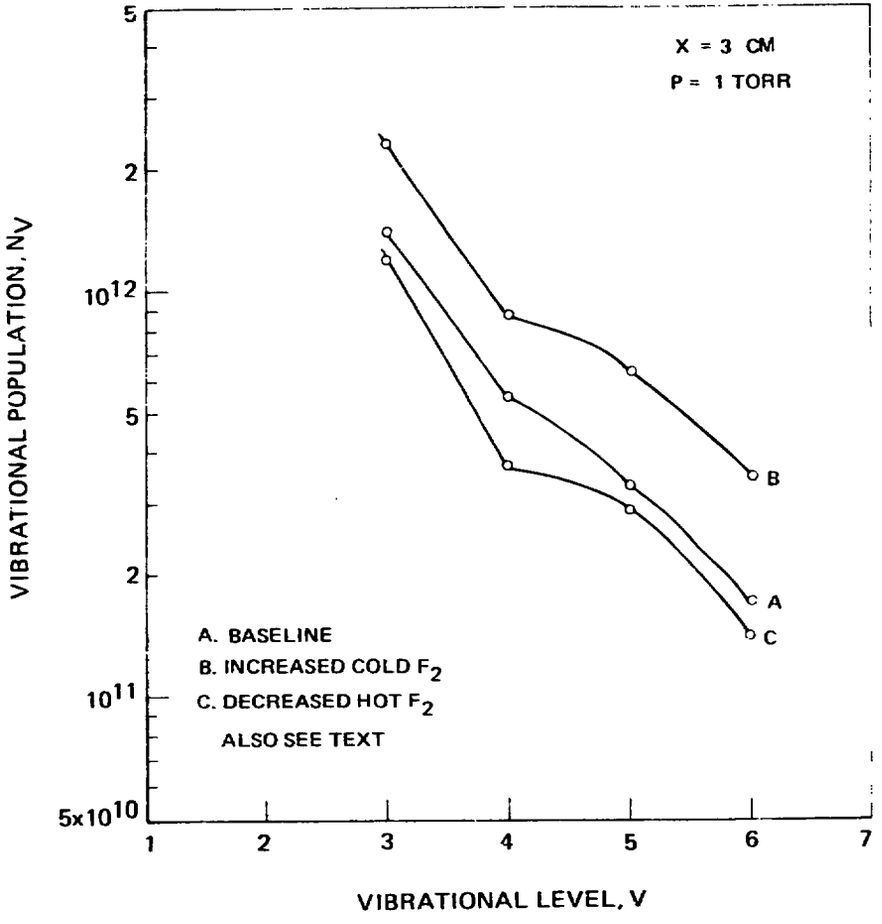

ANALYTICAL

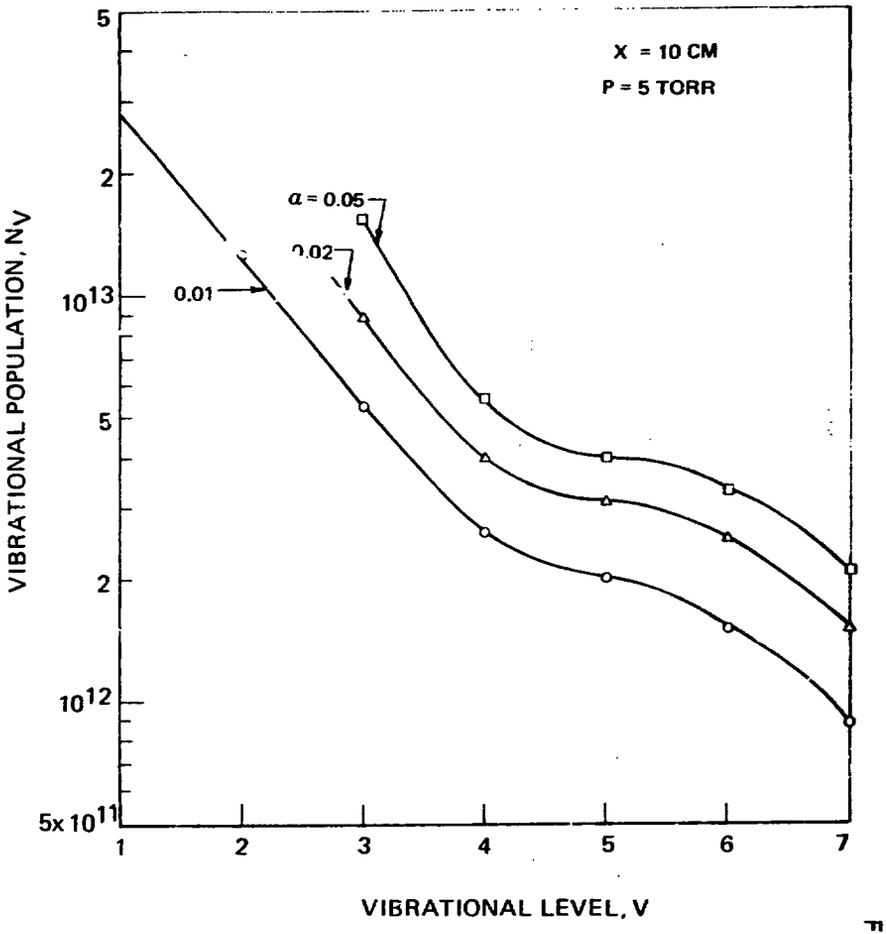

FIG. 14

of 2. The interesting point about these data is the departure from a Boltzmann vibrational distribution, as demonstrated by the bump in these curves. Even more interesting is the comparison of this data with the existing model predictions shown in the right-hand side of Fig. 14. Although the absolute values and pressures are not equal, the bumps seen in both figures for the V = 5 and 6 levels is encouraging.

Effect of Reaction Tube Wall Material on Spatial N_V Distribution

A summary of experimental results at 5 torr pressure is shown in Fig. 15, including results with a teflon liner inserted inside the copper flow tube reactor and the prior data (Fig. 13) with the copper tube exposed-coefficient. Teflon has a much lower wall recombination for H atoms than copper (Ref. 24) and also would lead to less HF(V) deactivation. Some effects of optical reflection from teflon into the spectrometer may be present in these data. This would shift the points at x = 8, 21 and 41 cm down slightly, but nevertheless relative effects such as the observed level population reduction with increasing level between v = 3 and 6 appear valid and only slightly changed by wall material. Between 8 and 21 cm the teflon wall results do not exhibit as sharp a drop off in population for all levels as is seen in the copper wall data. Also, a somewhat reduced rate of reduction in populations is indicated with the teflon. This suggests that H atom diffusion to the wall and wall recombination has had a measurable effect on the copper wall data. The observed effects here are larger than would be expected from a rough estimate of H atom diffusional loss rate compared to the hot reaction rate of H with F_2 but a review of the topic including more accurate calculations would appear worthwhile. Diffusional loss of HF(V) to the walls would be much lower than H atom diffusion and should not be significant here.

The rotational temperature spatial distributions inferred from emission data are shown inFig. 16a for the teflon wall and Fig. 16b for the copper wall. The teflon wall has resulted in reduced scatter of rotational temperature data and a somewhat enhanced buildup of temperature and reaction. Again wall loss of H atoms with the present optical depth of field appears to have had a measurable effect on the copper wall.

AVAILABLE EXPERIMENTAL RESULTS AT 5 TORR ON THE DISTRIBUTION OF HIGH LYING HF VIBRATIONAL LEVEL POPULATIONS IN THE F_2/H_2 CHAIN REACTION FLOW TUBE

NOMINAL CONDITIONS: $X_{F_2} = 1\%$; $X_{H_2} = 3\%$; $v = .10^4$ CM/SEC;
DISSOCIATION TUBE HEATER SETTING, $T_D = 640^oC$

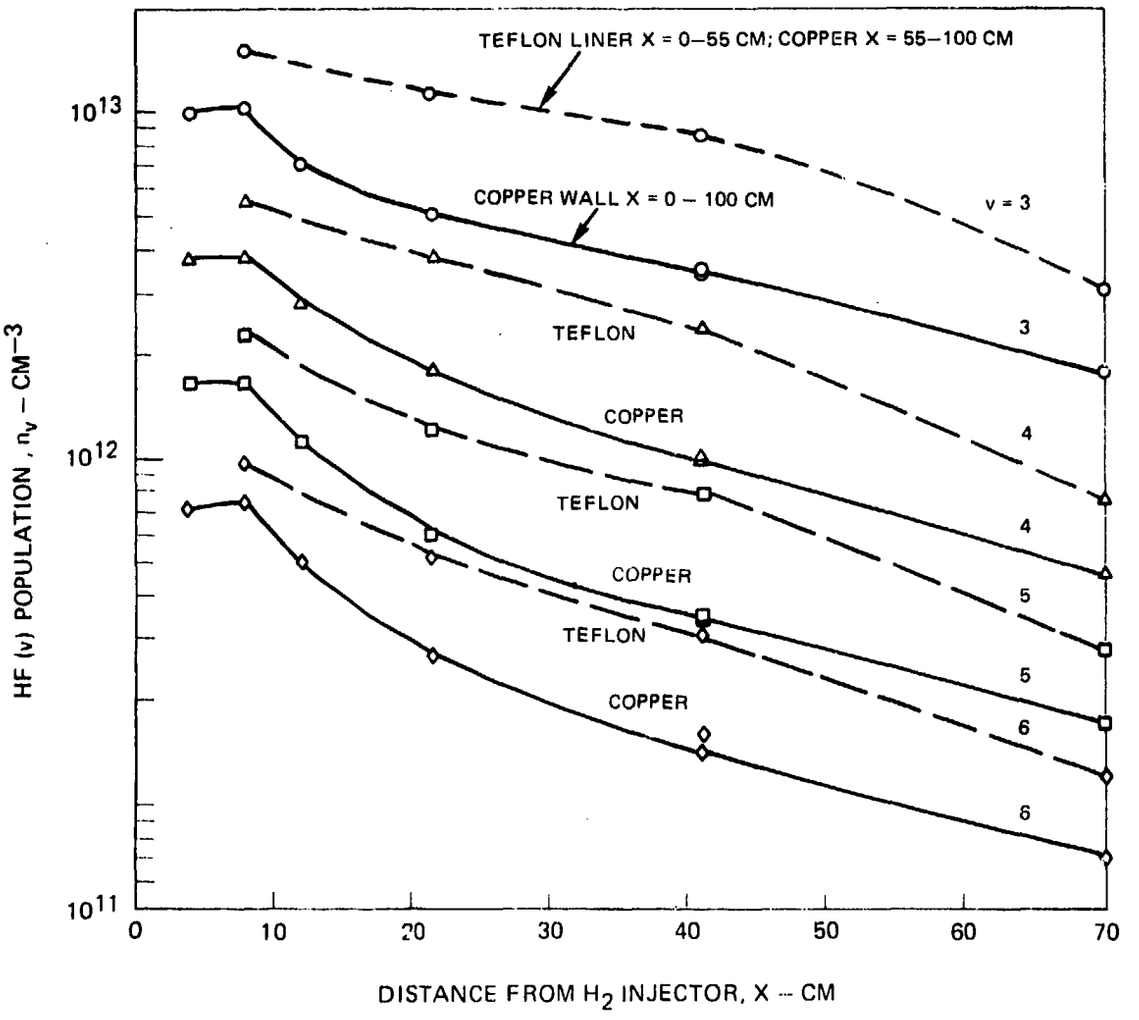

NOTES 1) ABSOLUTE POPULATION LEVELS ARE PRELIMINARY
SINCE WALL AND WINDOW REFLECTION FACTORS HAVE
NOT BEEN APPLIED TO OVERTONE EMISSION INTENSITY DATA AS YET

2) ULTRA HIGH PURITY H_2 AND Ar GAS CHECKS:
NO CHANGE IN EMISSION AT SELECTED POINTS WHEN BASELINE DRY H_2 AND
H.P. Ar SWITCHED SEPARATING TO HIGHER PURITY GRADES.
COMBINED TEST NOT AVAILABLE AT PRESENT

R05-38-2

FIG. 15

AVAILABLE EXPERIMENTAL RESULTS AT 5 TORR ON THE DISTRIBUTION OF HIGH LYING HF VIBRATIONAL LEVEL POPULATIONS IN THE F_2/H_2 CHAIN REACTION FLOW TUBE

NOMINAL CONDITIONS: X_{F_2} = 1% ; X_{H_2} = 3%; v = 10^4 CM/SEC;
DISSOCIATION TUBE HEATER SETTING, T_D = 640°C

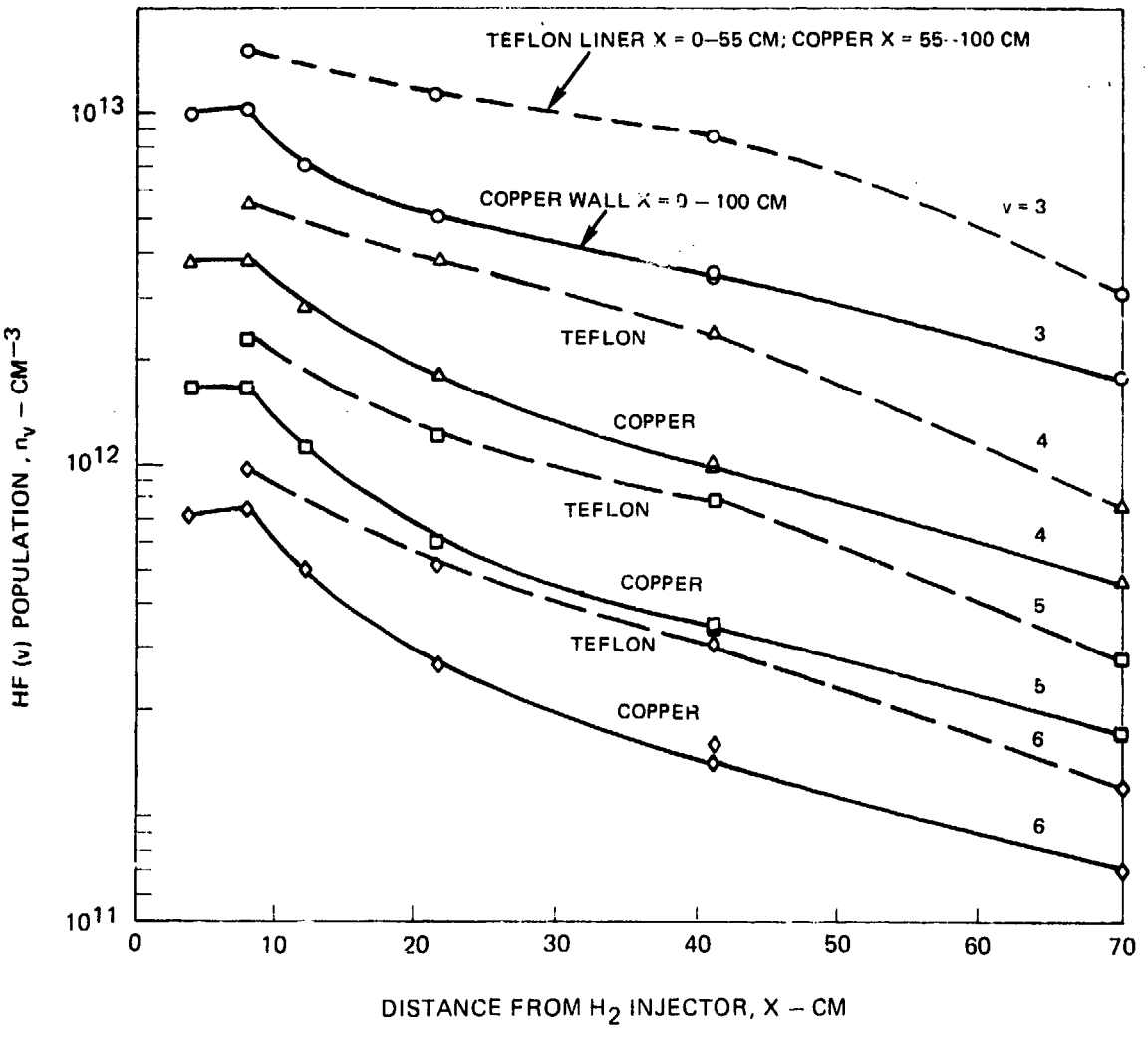

NOTES 1) ABSOLUTE POPULATION LEVELS ARE PRELIMINARY
SINCE WALL AND WINDOW REFLECTION FACTORS HAVE
NOT BEEN APPLIED TO OVERTONE EMISSION INTENSITY DATA AS YET

2) ULTRA HIGH PURITY H_2 AND Ar GAS CHECKS:
NO CHANGE IN EMISSION AT SELECTED POINTS WHEN BASELINE DRY H_2 AND
H.P. Ar SWITCHED SEPARATING TO HIGHER PURITY GRADES.
COMBINED TEST NOT AVAILABLE AT PRESENT

R05--38--2

FIG. 16

EFFECT OF WALL MATERIAL ON ROTATIONAL TEMPERATURE EXPERIMENTAL RESULTS

NOMINAL CONDITIONS: P = 5 TORR; X_{F_2} = 1%; X_{He} = 3%; DISSOCIATION TUBE HEATER SETTING, T_D = 640°C

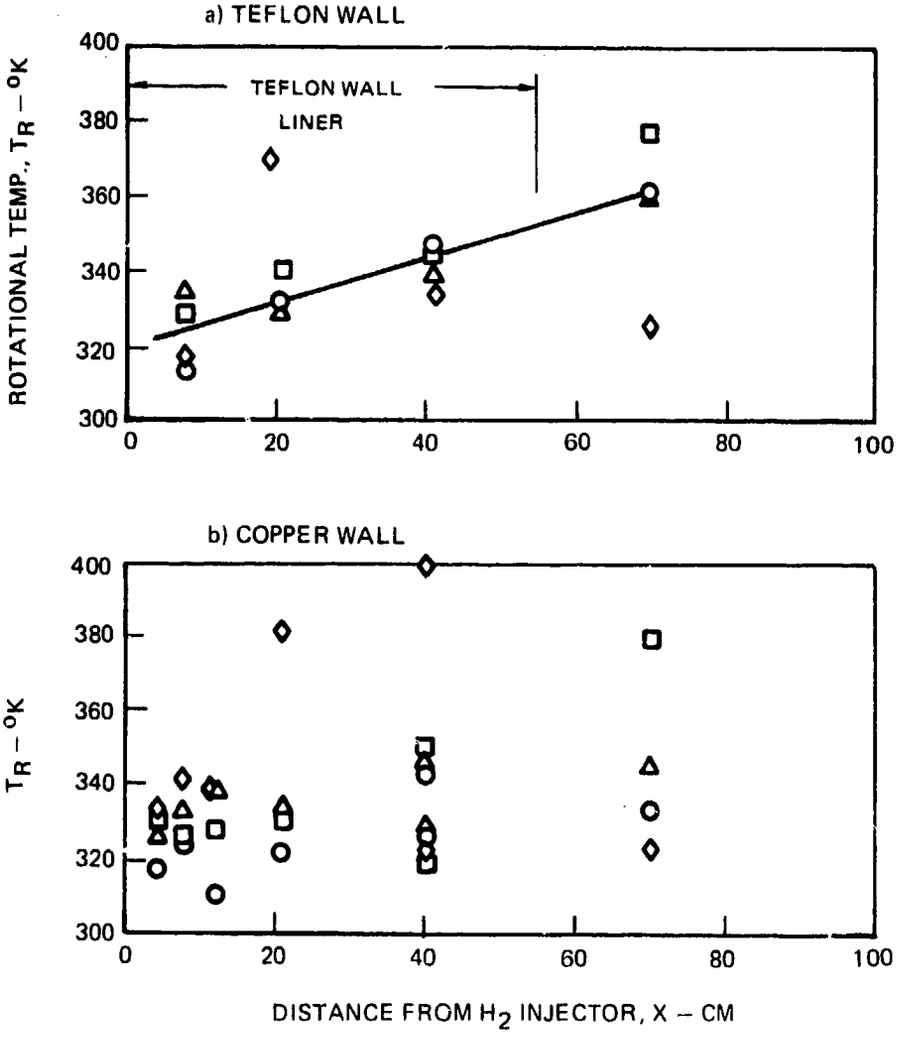

SYM	Δv DATA
○	3 → 0
□	4 → 1
△	5 → 2
◇	6 → 3

R05–38–3

VII. ONE-DIMENSIONAL KINETIC MODEL FOR THE F_2/H_2 CHAIN REACTION

Theoretical Model

Theoretical population profiles were generated from the solution to the following set of kinetic master equations ($x > l_{mix}$):

$$\frac{d(n_r u)}{dx} =$$

$$\frac{d}{dx}(n_r u) = \sum_q \left(K^{(r)}_{f,q} N_i N_j - K^{(r)}_{b,q} N_K n_r \right) \qquad \text{(chemical pumping)}$$

$$+ \sum_\ell \left(P^{\ell,\ell-1}_{r+1,r} \; n_{r+1} n_\ell - P^{\ell-1,\ell}_{r,r+1} n_r n_{\ell-1} \right) \quad - \sum_\ell \left(P^{\ell,\ell-1}_{r+1,r} \; n_{r+1} n_\ell - P^{\ell+1,\ell}_{r-1,r} \; n_r n_{\ell+1} \right) \qquad \text{(intramolecular VV exchange)}$$

$$+ \sum_\ell \left(Q^{\ell,\ell-1}_{r+1,r} \; n_{r+1} \hat{n}_\ell - Q^{\ell-1,\ell}_{r,r+1} n_r \hat{n}_{\ell-1} \right) \quad - \sum_\ell \left(Q^{\ell,\ell+1}_{r,r-1} \; n_r \hat{n}_\ell - Q^{\ell+1,\ell}_{r-1,r} \; n_{r-1} \hat{n}_{\ell+1} \right) \qquad \text{(intermolecular VV exchange)}$$

$$+ \sum_m \left(R^{(m)}_{r+1,r} \; N_m n_{r+1} - R^{(m)}_{r,r+1} N_m n \right) \quad - \sum_m \left(R^{(m)}_{r,r-1} \; N_m n_r - R^{(m)}_{r-1,r} \; N_m n_{r-1} \right) \qquad \text{(VT relaxation)}$$

$$+ A_{r+1,r} \; n_{r+1} - A_{r,r-1} n_r \qquad \text{(spontaneous emission)}$$

where n_r is the number density of the HF(v=r) state, $\hat{n}_\ell$ is the number density of the $H_2(v=\ell)$ state, and N_i is the number density of the ith chemical species (e.g., H, F, F_2, Ar, $\sum_v HF(v)$, $\sum_v H_2(v)$). The q summation is over all chemical reactions involving the vibrational state r (in the calculations to follow, just the hot and cold reactions); the ℓ summation is over all vibrational states, and the m summation over all chemical species. The symbols K,P, Q and R denote appropriate constants, and A the spontaneous emission coefficient. Detailed balance is employed to calculate all reverse rate coefficients, viz:

$$P^{\ell-1,\ell}_{r,r+1} = P^{\ell,\ell-1}_{r+1,r} \exp\left(-\left(E_{r+1} - E_r + E_\ell - E_{\ell-1}\right)/kT\right)$$

$$Q^{\ell-1,\ell}_{r,r+1} = Q^{\ell,\ell-1}_{r+1,r} \exp\left(-\left(E_{r+1} - E_r + F_\ell - F_{\ell-1}\right)/kT\right)$$

$$R^{(m)}_{r,r+1} = R^{(m)}_{r+1,r} \exp\left(-\left(E_{r+1} - E_r\right)/kT\right)$$

where E_r and F_s denote the energies of the HF and H_2 states, respectively.

The major assumption involved in deriving the kinetic equations is that of single quantum relaxation steps. Inviscid, constant area flow is assumed in deriving the flow velocity derivative.

Analogous equations are written for the H_2 vibrational state populations, and the coupled set of differential equations is integrated using an implicit, centered-difference scheme.

Rate Coefficients

Reviews of the kinetics literature relevant to HF chemical lasers have been given by Cohen (Refs. 25, 26). Rate coefficients for chemical processes and all relaxation processes affecting HF(v=1) are in essential agreement with the most recent recommendations (Ref. 26). One exception, however, is the treatment of the "back" cold reaction

$$H + HF(V) \underset{K_V}{\overset{K\text{-}V}{\rightleftarrows}} H_2 + F \quad \text{for} \quad V = 3, 4, 5, 6, 7$$

In the UTRC code, it is assumed that the product H_2 is in the ground state. K_{-3} is obtained by simple applying detailed balance to the known rate K_3. For $v \geq 4$, it is assumed that these processes proceed with zero activation energy, which results in a value of approximately 3×10^{-10} cm^3/molecule/sec for all levels. This is essentially a "gas kinetic" rate, and probably represents a reasonable upper bound. These processes do not appear to be important for the flow tube conditions investigated thus far.

The UTRC model scales the HF-HF VV in accordance with the following simple functions:

$$P^{s,s+1}_{r,r-1} \alpha\ r(s+1)\ T^{-1} \exp\ (-C/\Delta E^2) \exp\ (\frac{\Delta E}{2KT})$$

Several investigators have reported rate coefficient values for $P^{0,1}_{r,r-1}$ (Refs. 7, 8, 27). This data indicates that $P^{0,1}_{r,r-1}$ increases with r. There are discrepancies in the data for the higher quantum numbers; however, it is not clear that the data can be identified with VV exchange only, and contributions from other loss processes may be important. In view of this uncertainty, it is difficult to know how to get the theoretical expression for the data. We have therefore chosen a value of C such that the rate constants $P^{0,1}_{r,r-1}$ $2 \leq r \leq 6$ are only weakly dependent on r, i.e.,

$$P^{0,1}_{r,r-1} \simeq P^{0,1}_{2,1}$$

As will be seen this VV rate model correctly predicts the early "Boltzmannizing" of levels V = 3, 4, 5, 6 that is seen in the experiment. However, under conditions of low translational temperature and zero optical power output, use of these VV rates can cause truncations or bottleneck problems at the highest vibrational level considered (typically v = 12). This problem arises when a linear scaling of VT transition probabilities is assumed, and regardless of whether the HF-HF VV rates are truncated in magnitude at "gas kinetic" or ten times "gas kinetic". For faster HF-HF VT scaling, this problem disappears.

VIII. COMPARISON OF GENERAL FEATURES OF THE ANALYTICAL MODEL WITH EXPERIMENTAL RESULTS

Treanor Distribution in HF - the Limit of Dominant VV Transfer

Because there is a temptation to identify the distribution of Fig. (15) with "VV equilibrium" it is of interest to consider what the true VV equilibrium distribution of vibrational level populations in HF would be i.e., dominant VV transfer, for vibrational and translational/rotational temperatures consistant with the observed data, Fig. 15. Such a "Treanor" type distribution (Ref. 28) for HF is shown in Fig. 17, and it is apparent that the anharmonic nature of HF would result in a strong pumping of population to high lying levels when in fact the data, Fig. 15, show that reduced population at high lying levels is actually observed. If one examines the leading master equation terms describing VV pumping between any two levels (say v=4, and v=5) and assumes the approximate validity of the VV rates reported in the literature it becomes apparent that the population distributions of Fig. 15 represent a situation in which there should be strong anharmonic pumping from the lower to the higher levels. The fact that the measured populations decrease with distance indicates that there is some loss process which dominates the VV pumping. As will be seen, the loss rates in present, accepted use are not sufficiently rapid to compete with these VV pumping processes. It is also possible that these VV processes are not as efficient as reported in the literature.

Modeling of the Experiment

Calculations with the 1-D computer model have been made using conditions corresponding approximately to the actual conditions of the experiment. An initial dissociation fraction of F_2, $\alpha_{F_2} = 0.5\%$ has been employed. This value was chosen considering a limit provided by available uv absorption data $0 \leq \alpha_{F_2} \lesssim 2\%$ and the observation that if α_{F_2} were less than 0.5% it would be difficult to explain the high vibrational population levels observed close to the injector. The fact that a value of α_{F_2} close to the anticipated lower limit has been chosen rather than in between the limits has been motivated by a desire to see if calculated values of translational temperature buildup could be matched to the slow observed rotational temperature buildup along the flow tube without having to introduce inhibitor or other arguments. Further experimental information on α_{F_2} particularly a lower limit type of measurement is needed. The concentration of F_2 for the nominal 1% case, (Fig. 15) after calibration of flowmeters and consideration of purge and boundary layer injectant inert gas flows was found to correspond actually to $X_{F_2} = 0.018$ near the H_2-injector and would be $X_{F_2} = 0.012$ far downstream after all auxillary inert flows had mixed in. Both values of X_{F_2} have been used in the model in an effort to bracket the results although a more detailed treatment of the boundary

FIG. 17

TREANOR DISTRIBUTION IN HF

$$\frac{N_{v+1}}{N_v} = \exp\left\{ - \frac{(E_1 - E_0)}{KT_1} + 2v\omega_e X_e \frac{hc}{KT} \right\}$$

$T_1 = 5000^\circ K$; $T = 400^\circ K$

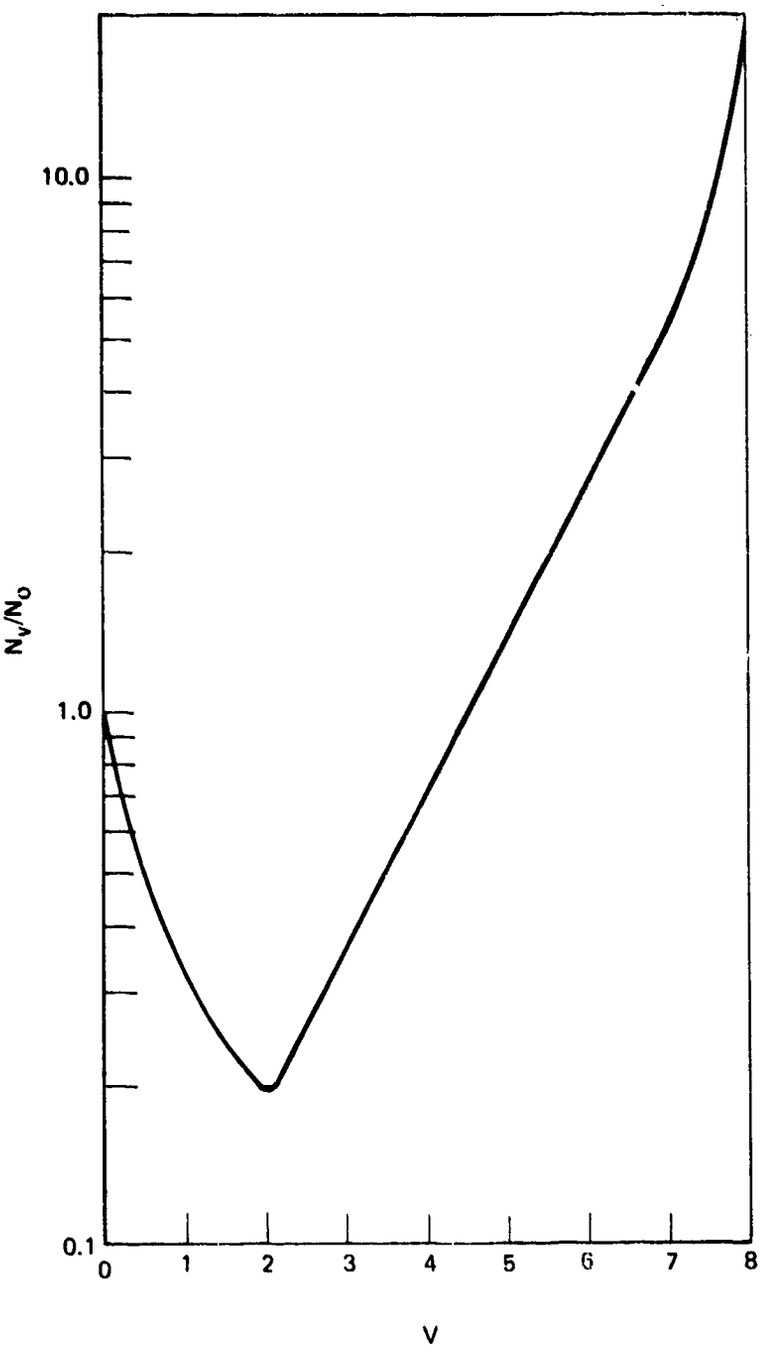

R05-38-4

layer/mixing region at the wall is needed or preferably, a reduction in optical depth of field relative to tube diameter to exclude emission originating near the wall from the observed intensities. Based on flowmeter calibrations the nominal H_2 concentration of 3% was found to be $^{X}H_2 = 0.024$ relative to all flows and because of the faster diffusion of H_2 this value has been used to represent the entire flow tube region. Measured pressure p actually varied from about 5.5 torr to 4.5 torr along the 1 meter flow tube for the flow rates employed and p = 5 has been used as a good approximation at this time. Velocity $V=10^4$ cm/sec is close to the actual value based on measured flows and pressure. Actual velocity would be somewhat less near the injector and somewhat higher near the end of the tube due to the pressure variation/boundary layer process but again no attempt to account for this variation is warranted for purposes of the present comparison. Note that the Mach number of the flow relative to Ar thermal speed at T = 300°K is M ~ 0.3, a moderate subsonic condition.

Slight surface reaction patterns have been observed on the H_2 injector tubes and these give an indication of mixing effectiveness. These patterns indicate that penetration of the H_2 + Ar angled injectants from the orifices across the flow tube reactor is occurring close tothe injector as desired in a uniform manner and that sufficient momentum is present in the F_2 + Ar flow to prevent backstreaming of the H_2 + Ar injectant. Rapid uniform mixing of H_2 and F_2 would be expected for this angled injector geometry in a distance $X_{mix} \leq 5$ cm for an injectant orifice spacing of 1.5 mm. The detailed mixing profile with distance has not been included in the cases that have been examined with the model since it is short relative to the observation length and not expected to have a significant effect on interpretation of results.

Predicted Results with Present Models of Back Reaction, H_2-HF and HF-HF Interaction

Predicted results for $^{X}F_2 = 0.018$ are shown in Fig. 18 with kinetic mechanisms describing back reaction, H_2 - HF and HF-HF interactions treated in the existing manner including a linear HF-HF VT scaling with V. The dashed lines indicate the expected results if the hot reaction never occurred. A comparison with the data, Fig. 15, suggests that the hot reaction is occurring in theexperiment and vibrational levels are being populated by the chain. The experimental observation that increased cold F_2 addition after the dissociator leads to increased emission intensities also indicates that the hot reaction and chain are occurring. The solid lines in Fig. 18 are predicted results for the chain. The predicted populations are of the same order as measured values but the predicted distribution with V shows higher and near equal populations for V = 4, 5, 6 while the measurements, (Fig. 15) show a substantial dropoff in populations with increasing V. The predicted populations begin to rise downstream because the rates of change due to hot reaction pumping are increasing with distance. Strong anharmonic pumping due to HF-HF VV exchange is also present. Significantly, the theoretical model correctly predicts that the populations close

FIG. 18

PREDICTED I-D VIBRATIONAL LEVEL POPULATIONS IN CHAIN REACTION WITH LINEAR HF-HF VT SCALING WITH V

BASELINE BACK REACTION AND H_2 HF VV MODELS

P = 5 TORR, T = 300°K, v ~ 10^4 cm/sec

X_{F_2} = 1.8%, X_{H_2} = 2.4%

FLUORINE DISSOCIATION, α_{F_2} = 0.5%

X_{MIX} = 0.1 CM

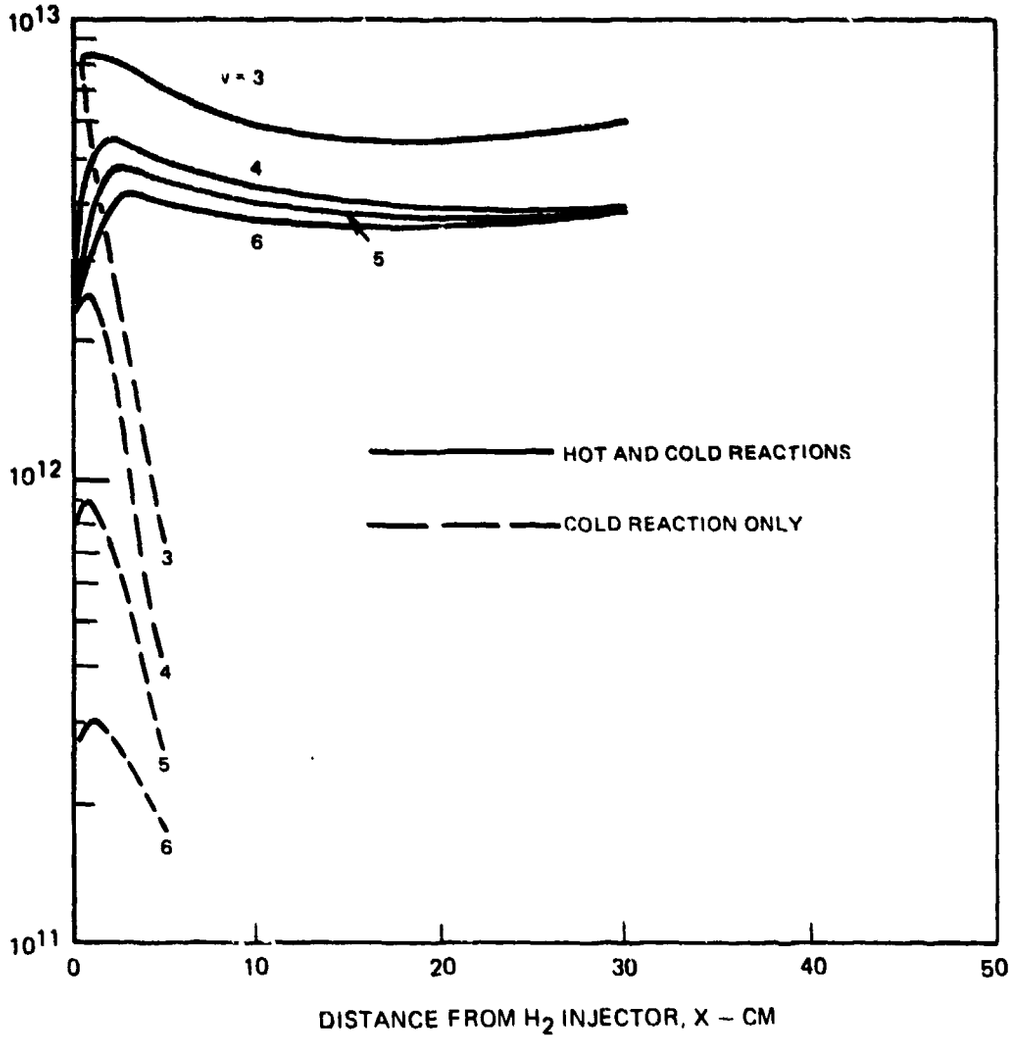

R05-38-1

to the injector should be approximately Boltzmann, as is seen in the experiment. The initial measured and calculated populations are far from the hot reaction primitive distributions for this pressure level. This suggests that the HF-HF VV rates in the code are approximately correct.

Predicted Results with Increased Loss Rates of High Lying Levels

In trying to relate the above discrepancy to potential kinetic uncertainties in the model reasonable increases in back reaction, H_2-HF VV and HF-HF VT processes were tried. Increase in an already fast HF(V) back reaction process with H by a factor of 10 produced only about an order 10% reduction in V = 4, 5, 6, populations. Speed-up in coupling of H_2 with HF levels while possible for lower levels would not have a significant effect on upper level population, moreover, the observed effects of H_2, Table 3, appear to be predicted reasonably well by the model. In the calculations H_2 is pumped via HF-H_2 VV exchange to a vibrational temperature of about 2000°K. It appears that most of this energy transfer is from the lower HF vibrational states; because of favorable energetics, excited H_2 can pump energy back into the higher HF states ($v \geq 4$). Based on the H_2 VT rates in use in the code (Refs, 25, 26) little H_2 relaxation is predicted. Speed-up in the HF-HF VT deactivation of high lying levels by increased scaling with V was tried and the results for a V^3 scaling, Fig. 19 yield a much closer correlation of predicted and measured results on level population distribution with level. The HF-HF VT rates were truncated at 10^7 sec^{-1} $torr^{-1}$ for the higher levels. The absolute level of populations predicted for X_{F_2} = 1.8%, Fig. 19a, appear high relative to data Fig. 15 while predicted results for X_{F_2} = 1.2% and a slow hot reaction rate appear more reasonable. The base rate constant for the hot reaction is the value reported by Albright (Ref. 2).

Overall Reaction Rate, Gas Temperature Increase

The translational temperature increases predicted by the model as the chain reaction developes are shown in Fig. 20 for the two F_2 concentrations and baseline and slow H + F_2 reaction rates. The slope of the average line through the rotational temperature data of Fig. 16a is included in Fig. 20. The comparison suggests that the overall reaction may be proceeding somewhat slower than predicted, accounting for some of the discrepancy between predicted and measured vibrational population levels.

EFFECT OF V^3 HF–HF VT SCALING WITH V ON PREDICTED 1–D CHAIN REACTION VIBRATIONAL LEVEL POPULATIONS

BASELINE BACKREACTION AND H_2–HF VV MODELS

a) X_{F_2} = 1.8%

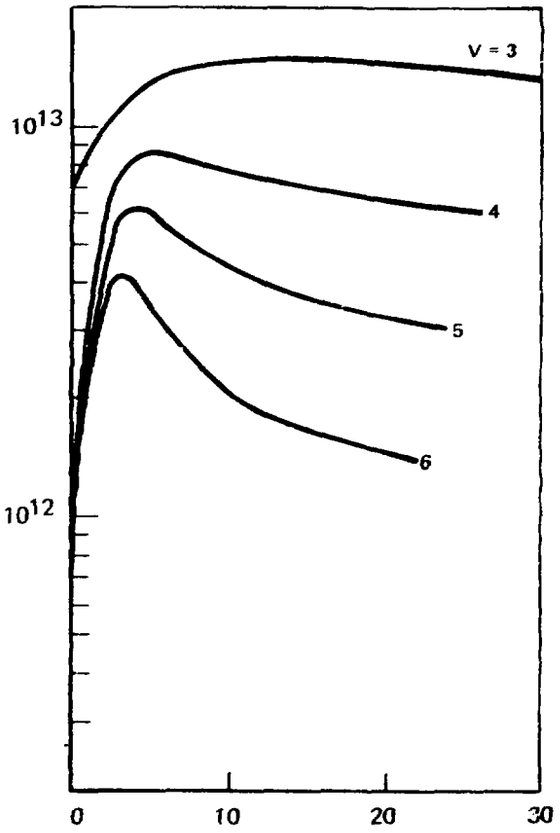

DISTANCE FROM H_2 INJECTOR, X – CM

b) X_{F_2} = 1.2%

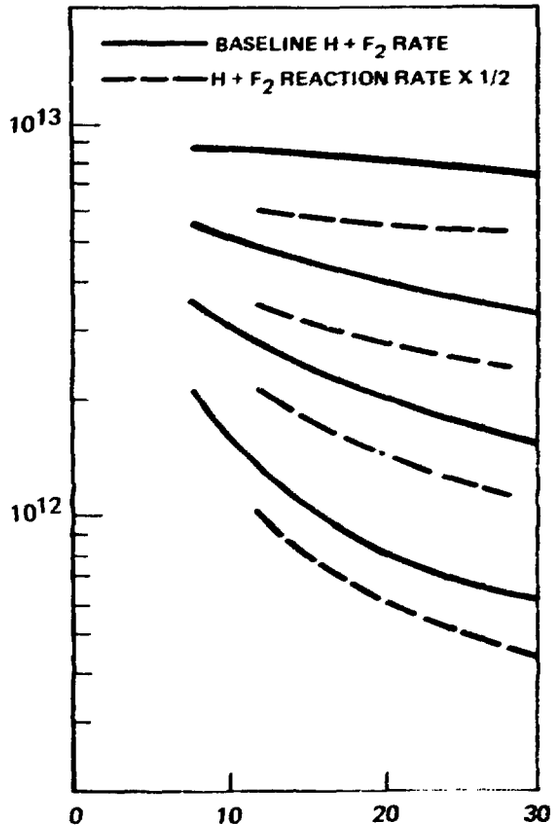

DISTANCE FROM H_2 INJECTOR, X – CM

FIG. 19

PREDICTED I–D TRANSLATIONAL TEMPERATURE RISE IN CHAIN REACTION

V^3 HF–HF VT WITH V

BASELINE BACKREACTION AND H_2–HF VV MODELS

P = 5 TORR v = 10^4 M CM/SEC

X_{H_2} = 2.4%

FLUORINE DISSOCIATION, α_{F_2} = 0.5%

X_{MIX} = 0.1 cm

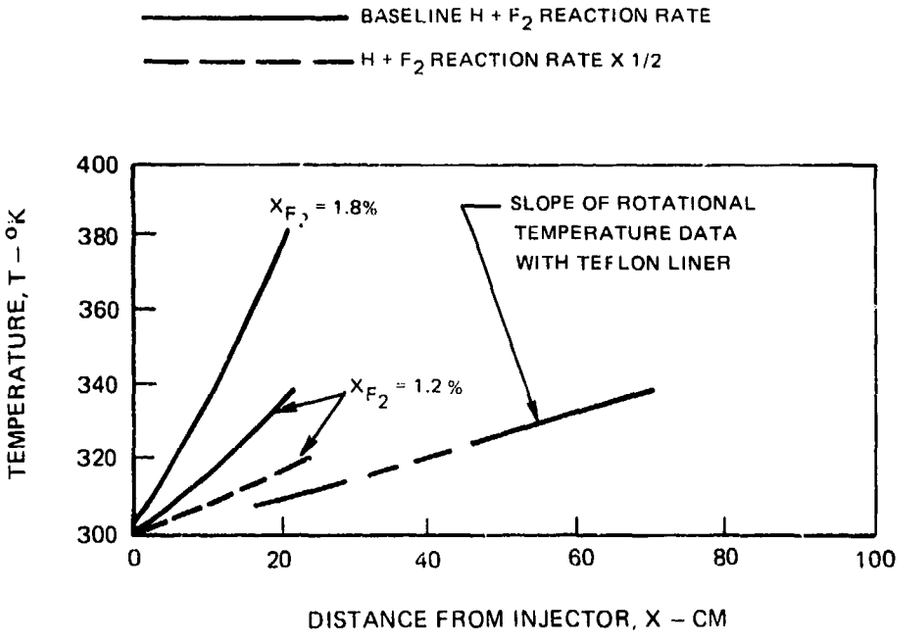

R05–38–5

IX. CONCLUSIONS

The results of this study indicate: 1) The thermally initiated F_2/H_2 flow tube reactor experiment, designed, fabricated and tested under this contract is a viable approach for providing information on HF chain reaction and relaxation kinetics for comparison with existing codes, 2) Key areas of kinetic uncertainty with the chain appear to exist - in particular, the experimental results when compared with the model suggest a) HF-HF VV and VT processes are uncertain and b) the overall rate of reaction and translational heating may be uncertain.

X. RECOMMENDATIONS

The above results are not conclusive at this time, lacking sufficient checks and detail for final definitive adjustment of the model. Additional information needed includes better definition of the initial F-atom concentration, population measurements of HF in the v=0, 1 and 2 states and an assessment of the effects of H and F atoms diffusion and interaction with the walls. More extensive low pressure data and the effect of HF(0) addition are also required to provide experimental information on HF-HF interactions. Further information on the overall production of HF and the resulting translational heating is also needed. Finally, the effects of possible oxygen contamination of the fluorine and of temperature variations on the overall reaction rate also need further investigation.

XI. ACKNOWLEDGMENTS

The authors wish to acknowledge the support and guidance in the initial phases of this work of Barry R. Bronfin who as Principal Scientist, Nonequilibrium Chemical Reactions initiated the study. The authors also wish to acknowledge the support and encouragement of the work at this time by Casper J. Ultee, Principal Scientist, Atomic and Molecular Structure.

REFERENCES

1. Homann, K. H., et al: Eine Methode zur Erzeugung von Fluoratomer in Inerten Atmosphäre. Ber. Bunser. F. Phys. Chem. 74, 585 (1970).

2. Albright, R. G., et al: Mass-Spectrometric Determination of Rate Constants for H-Atom Reactions with Cl_2 and F_2. J. Chem. Phys. 50, 3632 (1969).

3. Jonathan, N., et al: Initial Vibrational Energy Level Distributions Determined by Infrared Chemiluminescence. Mol. Phys., 22, 561 (1971).

4. Jonathan, N., C. M. Melliar-Smith and D. H. Slater: Initial Vibrational Energy Level Populations Resulting from the Reaction H + F_2 as Studied by Infrared Chemiluminescence. J. Chem. Phys., 53, 4396 (1970).

5. Polanyi, J. C. and K. B. Woodall: Energy Distribution Among Reaction Products VI F + H_2, D_2. J. Chem. Phys., 57, 1574 (1972).

6. Polanyi, J. C. and J. J. Sloan: Energy Distribution Among Reaction Products VII H + F_2. J. Chem. Phys., 57, 4988 (1972).

7. Airey, J. R. and I. W. M. Smith: Quenching of Infrared Chemiliminescence: Rates of Energy Transfer from HF ($v \leq 5$) to CO_2 and HF, and from DF ($v \leq 3$) to CO_2 and HF. J. Chem. Phys., 57, 1669 (1972).

8. Wilkins, R. L., M. A. Kwok, N. Cohen, and J. F. Bott: Vibrational Energy Transfer Among Upper Vibrational Levels of HF (v). Presented at the Tri-Service Chemical Laser Symposium, 19-21 February 1975, Kirtland Air Force Base, New Mexico.

9. Kwok, M. A. and R. L. Wilkins: Flow Tube Measurements of H + HF(v) Deactivation Rates. J. Chem. Phys., 60, 2189 (1974).

10. Stedman, D. and D. H. Stetser: Progress in Reaction Kinetics, Vol. 6, Part 4, Pergamon Press, Oxford, England, 1972.

11. Suchard, S. N., L. B. Bergerson: Fluorine Pressure Change Monitor for a Reacting System. Rev. Sci. Inst., 43, 1717 (1972).

12. Suchard, S. N. and D. G. Sutton: Laser Actinometry of Flash-Photolyzed $H_2/F_2/He$ Mixtures. IEEE J. Q. E., QE-10, 490 (1974).

13. JANAF "Thermochemical Tables", Sept. 1965.

14. Bender, L. S., R. J. Tripodi and B. R. Bronfin: Selected Physic-Chemical Data for the Hydrogen-Fluorine Chemical Laser. UAR-127, March 1972.

References (Cont'd)

15. Ultee, C: UTRC internal reports on ESR studies of F-atom Surface Recombination.

16. Steunenb[illegible] F. K., R. C. Vogel: The Absorption Spectrum of Fluorine. J. Am. Chem. So... 78, 901 (1956).

17. Ro[illegible] A. L. G.: Electronic Spectrum and Dissociation Energy of Fluorine. J. Chem. Phys., 26, 567 (1957).

18. Meredith, R. E. and F. G. Smith: Investigations of Fundamental Laser Process, Vol. II, Sponsored by Advanced Projects Agency under Contract DAHC-75-67-C-0062, November 1971.

19. Proch, D. and J. Wanner: Tables of Vibrational-Rotational Transitions in Diatomic Molecules Pertinent to Chemical Lasers, Max Planck Institut für Plasma-physik, Garching bei München, March 1971.

20. Sileo, R. N.: Thesis, Cornell University, January 1974.

21. Rosen, D. I., R. N. Sileo, T. A. Cool: A Spectroscopic Study of CW Chemical Lasers, IEEE Journal of Quantum Electronics, QE-9, January 1973.

22. Levy, J. B., B. K. W. Copeland: The Kinetics of the Hydrogen-Fluorine Reaction III. The Photochemical Reaction. J. Chem. Phys., 729 (1968).

23. Parker, J. V. and R. R. Stephens: Chemical Laser Pulse Initiation Study. Hughes Research Laboratories, AFWL -TR-72-230, May 1973.

24. Wood, B. J. and H. Wise: Kinetics of Hydrogen Atom Recombination on Surfaces. J. Chem. Phys., 65, 1976 (1961).

25. Cohen, N. and J. F. Bott: Kinetics of Hydrogen Halide Chemical Laser Systems, Chemical Lasers, ed. R. W. F. Gross and J. F. Bott, Wiley Interscience (1975). (In press.)

26. Cohen, N.: Review of Rate Coefficients for Reactions in the H_2-F_2 Laser System (Revised), Air Force Report No. SAMSO-TR-73-209.

27. Osgood, R. M., P. B. Scakett and A. Javan: Measurement of Vibrational-Vibrational Exchange Rates for Excited Vibrational levels ($2 \leq v \leq 4$) in Hydrogen Fluoride Gas. J. Chem. Phys., 60, 1464 (1974).

28. Treanor, C. E., J. W. Rich and R. G. Rehm: Vibrational Relaxation of Anharmonic Oscillators with Exchange-Dominated Collisions. J. Chem. Phys, 48, 1798 (1968).